

**ARTICLE****Freshwater Ecology**

# The salmonid and the subsurface: Hillslope storage capacity determines the quality and distribution of fish habitat

D. N. Dralle<sup>1</sup>  | G. Rossi<sup>2</sup> | P. Georgakakos<sup>2</sup> | W. J. Hahm<sup>3</sup>  |  
 D. M. Rempe<sup>4</sup> | M. Blanchard<sup>5</sup> | M. E. Power<sup>6</sup> | W. E. Dietrich<sup>7</sup> |  
 S. M. Carlson<sup>2</sup> 

<sup>1</sup>United States Forest Service Pacific Southwest Research Station, Davis, California, USA

<sup>2</sup>Environmental Science, Policy, and Management, University of California, Berkeley, California, USA

<sup>3</sup>Department of Geography, Simon Fraser University, Burnaby, British Columbia, Canada

<sup>4</sup>Department of Geological Sciences, University of Texas-Austin, Austin, Texas, USA

<sup>5</sup>U.S. Fish and Wildlife Service, Portland, Oregon, USA

<sup>6</sup>Department of Integrative Biology, University of California Berkeley, Berkeley, California, USA

<sup>7</sup>Department of Earth and Planetary Science, University of California Berkeley, Berkeley, California, USA

**Correspondence**

D. N. Dralle  
Email: [david.dralle@usda.gov](mailto:david.dralle@usda.gov)

**Funding information**

National Science Foundation,  
Grant/Award Numbers: CZP  
EAR-1331940, 1948857, 1948994, 1948997

**Handling Editor:** Andrew L. Rypel

**Abstract**

Water in rivers is delivered via the critical zone (CZ)—the living skin of the Earth, extending from the top of the vegetation canopy through the soil and down to fresh bedrock and the bottom of significantly active groundwater. Consequently, the success of stream-rearing salmonids depends on the structure and resulting water storage and release processes of this zone. Physical processes below the land surface (the subsurface component of the CZ) ultimately determine how landscapes “filter” climate to manifest ecologically significant streamflow and temperature regimes. Subsurface water storage capacity of the CZ has emerged as a key hydrologic variable that integrates many of these subsurface processes, helping to explain flow regimes and terrestrial plant community composition. Here, we investigate how subsurface storage controls flow, temperature, and energetic regimes that matter for salmonids. We illustrate the explanatory power of broadly applicable, storage-based frameworks across a lithological gradient that spans the Eel River watershed of California. Study sites are climatically similar but differ in their geologies and consequent subsurface CZ structure that dictates water storage dynamics, leading to dramatically different hydrographs, temperature, and riparian regimes—with consequences for every aspect of salmonid life history. Lithological controls on the development of key subsurface CZ properties like storage capacity suggest a heretofore unexplored link between salmonids and geology, adding to a rich literature that highlights various fluvial and geomorphic influences on salmonid diversity and distribution. Rapidly advancing methods for estimating and observing subsurface water storage dynamics at large scales present new opportunities for more clearly identifying landscape features that constrain the distributions and abundances of organisms, including salmonids, at watershed scales.

**KEY WORDS**

flow regime, hillslope hydrology, rivers, salmonid, storage capacity, stream temperature

This is an open access article under the terms of the [Creative Commons Attribution License](#), which permits use, distribution and reproduction in any medium, provided the original work is properly cited.

© 2023 The Authors. *Ecosphere* published by Wiley Periodicals LLC on behalf of The Ecological Society of America.

## INTRODUCTION

Riverine biota, including salmonids, depend on multiple facets of streamflow. Flow regime (the timing and magnitude of streamflow) determines the accessibility and hydraulic features of habitat and influences the timing of key life history events, such as migration and spawning (e.g., Beechie et al., 2006; Sykes et al., 2009). Stream temperature and riparian light environment impact habitat suitability, fish metabolism, prey productivity, and salmonid growth potential (e.g., Armstrong et al., 2021; Bilby & Bisson, 1992). Human-caused changes in land use and climate have impacted riverine flows, temperatures, and riparian characteristics, altering aquatic ecosystems globally (Lehner et al., 2011). Proper attribution of drivers of change, as well as the development of successful mitigation and restoration strategies for aquatic ecosystems, requires that we understand the physical controls of these elements at watershed scales (e.g., Quinn et al., 1997; Sturrock et al., 2019).

Although climate strongly influences light environment, temperature, and water quantity and quality (e.g., Bergmeijer et al., 2020; Maurer et al., 2022), a full understanding of watershed function requires a critical zone (CZ) perspective, which integrates aboveground

processes (e.g., atmospheric fluxes, vegetation patterns, land use changes) with subsurface dynamics (infiltration, rooting zone processes, and weathering) and water storage (e.g., Anderson et al., 2007, 2008; Brantley et al., 2007; Grant & Dietrich, 2017; Riebe et al., 2016). In the upland freshwaters that host many rearing and spawning fish populations, water storage (as unsaturated storage in the vadose zone and as groundwater) in the subsurface CZ occurs in both the shallow soil layer (commonly <0.5-m thick) and deeper underlying layers of saprolite and weathered bedrock (Dawson et al., 2020; McCormick et al., 2021; Rempe & Dietrich, 2018; Wald et al., 2013).

The dynamic water storage capacity (storage capacity) of the subsurface CZ has emerged as an integrative catchment characteristic because of its ability to explain flow paths, flow generation, and plant community composition (Hahm, Rempe, et al., 2019; Illien et al., 2021; Klos et al., 2018; McDonnell et al., 2018; Sayama et al., 2011). A watershed's dynamic storage has been defined in various ways (e.g., Buttle, 2016; Dralle et al., 2018; Staudinger et al., 2017), but we here focus on a simple definition of the term: dynamic storage ( $\Delta S$ ; see terminology in Table 1) is the change in volume of water stored in a catchment relative to some reference storage state

**TABLE 1** Table of terminology.

GLOSSARY		
Term/quantity	Definition	Dimensions
Dynamic storage ( $\Delta S$ )	The volume of water stored in a catchment relative to some reference storage state, commonly taken to be zero at the driest time of year.	[L] or [ $L^3$ ]
Storage capacity	The maximum observed value of dynamic storage.	[L] or [ $L^3$ ]
Runoff ( $Q$ )	Stream discharge. Expressed in volumetric units (e.g., cubic meters per second), but also commonly reported in area-normalized units (e.g., millimeters per day) to facilitate runoff production intercomparisons between watersheds with different areas.	[L/T] or [ $L^3/T$ ]
Evapotranspiration	The sum of water use by vegetation (transpiration) and water returned to the atmosphere via evaporative losses from the ground surface or water bodies.	[L/T]
Recession timescale ( $\tau$ )	Determines the flow recession rate under the assumption that $Q$ decline is linearly proportional to $Q$ (i.e., $dQ/dt = -\frac{1}{\tau}Q$ ), leading to an exponential functional form for the streamflow recession.	[T]
Light penetration index	The number of light detection and ranging (LiDAR) returns from the ground or water surface divided by the total number of LiDAR returns.	Unitless
Runoff ratio	The ratio of total stream discharge to total precipitation over some time interval. Typically expressed over annual or longer timescales.	Unitless
Drainage density	The length of stream channel per area of watershed.	[ $L^{-1}$ ]
Saturation overland flow	Overland flow that occurs when groundwater tables rise from below and intersect the ground surface, leading to runoff production via direct precipitation on saturated areas or water exfiltrating from the groundwater (return flow).	[L/T] or [ $L^3/T$ ]
Contributing area	Defined at a point, the total upstream watershed area draining all streams and hillslopes to that point.	[ $L^2$ ]

(Hahm, Rempe, et al., 2019) as inferred through mass balance:

$$\Delta S = P - Q - ET, \quad (1)$$

where  $P$ ,  $Q$ , and  $ET$  are precipitation, stream discharge, and evapotranspiration, respectively. In hilly and mountainous landscapes underlain by bedrock, water storage capacity in the subsurface is set by the depth of chemical and physical weathering fronts that alter fresh bedrock and generate matrix porosity and fractures capable of retaining and releasing water (e.g., Callahan et al., 2020; Holbrook et al., 2014; Klos et al., 2018; Pedrazas et al., 2021). These weathering processes, and therefore water storage capacity, depend on tectonics, climate, biota, and, importantly, the underlying bedrock geology (e.g., Riebe et al., 2016). Exactly determining the water storage capacity of a watershed is intractable, but it can be roughly estimated by calculating the maximum observed value of dynamic storage (Hahm, Rempe, et al., 2019). Storage capacity in the subsurface sets the maximum volume of water that can be stored for later use by vegetation. It also mediates how climate and evapotranspiration affect the timing and magnitude of groundwater recharge, and thus runoff generation and river flow regime features (Dralle et al., 2018; Klos et al., 2018). Calculation of dynamic storage using Equation (1) may be confounded by cryptic or unmeasured fluxes, such as interbasin flow. Additionally, the dynamics of  $\Delta S$  will depend on the particulars of climate over a period of record. For additional discussion on interbasin flows, different approaches and definitions for calculating catchment storage dynamics, and climatic controls on subsurface storage dynamics, we recommend Fan (2019), Staudinger et al. (2017), and Wang-Erlandsson et al. (2016).

Here, we propose that hillslope subsurface water storage capacity can explain between-catchment differences in stream hydrologic and energetic features that matter for salmonid life history. Importantly, this is not a difference in larger scale or regional aquifers tied to intrinsic properties of fresh bedrock. Rather, the variability occurs at the hill-slope scale and is tied to the weathering-driven development of the CZ, which depends on material properties of the bedrock.

We demonstrate the utility of storage-based frameworks for understanding watershed ecohydrological processes through a case study of California's Eel River, which has been designated by the California Department of Fish and Wildlife and State Water Resources Control Board as a priority salmonid conservation watershed. In *Geology, subsurface structure, and storage*, we synthesize results from a decade-plus effort

of subsurface monitoring enabled by deep drilling (Hahm et al., 2020; Rempe & Dietrich, 2018; Salve et al., 2012; Schmidt & Rempe, 2020; Tune et al., 2020) showing how subsurface structure and rock type explain variations in water storage capacity and plant community composition at two intensively monitored Eel River subcatchments. These sites are underlain by two different bedrock lithologies (the Coastal Belt turbidites and Central Belt melange of the Franciscan Complex) that have similar geochemical composition but have weathered differently (deep and shallow, respectively) because of different rock properties (Hahm, Rempe, et al., 2019). *Water storage dynamics and runoff* then explores how lithologically determined storage capacity drives differences in flow regime (Yarnell et al., 2020) and stream water availability at the scale of small catchments and larger sub-watersheds of the Eel River. Analogously to the section on water, *Energy budgets and stream temperature* focuses on how storage capacity can affect energy fluxes and temperature dynamics in stream channels. *Salmonids and the subsurface: Life history framework and hypotheses* brings together the water and energy budget results to generate testable hypotheses that aim to address how differences in hillslope water storage capacity affect stream-rearing salmonids—at specific life stages and holistically as life history syndromes. Our findings indicate that lithologically controlled storage capacity has widespread impacts on the spatial and temporal distribution of habitat quantity and quality, factors that influence the diversity of salmonid life histories. Finally, *Discussion* aims to link aspects of our findings to other important bodies of the literature, including approaches for measuring storage capacity, efforts to understand CZ controls on stream temperature, and potential linkages between the evolution of landscapes and salmon over geological timescales.

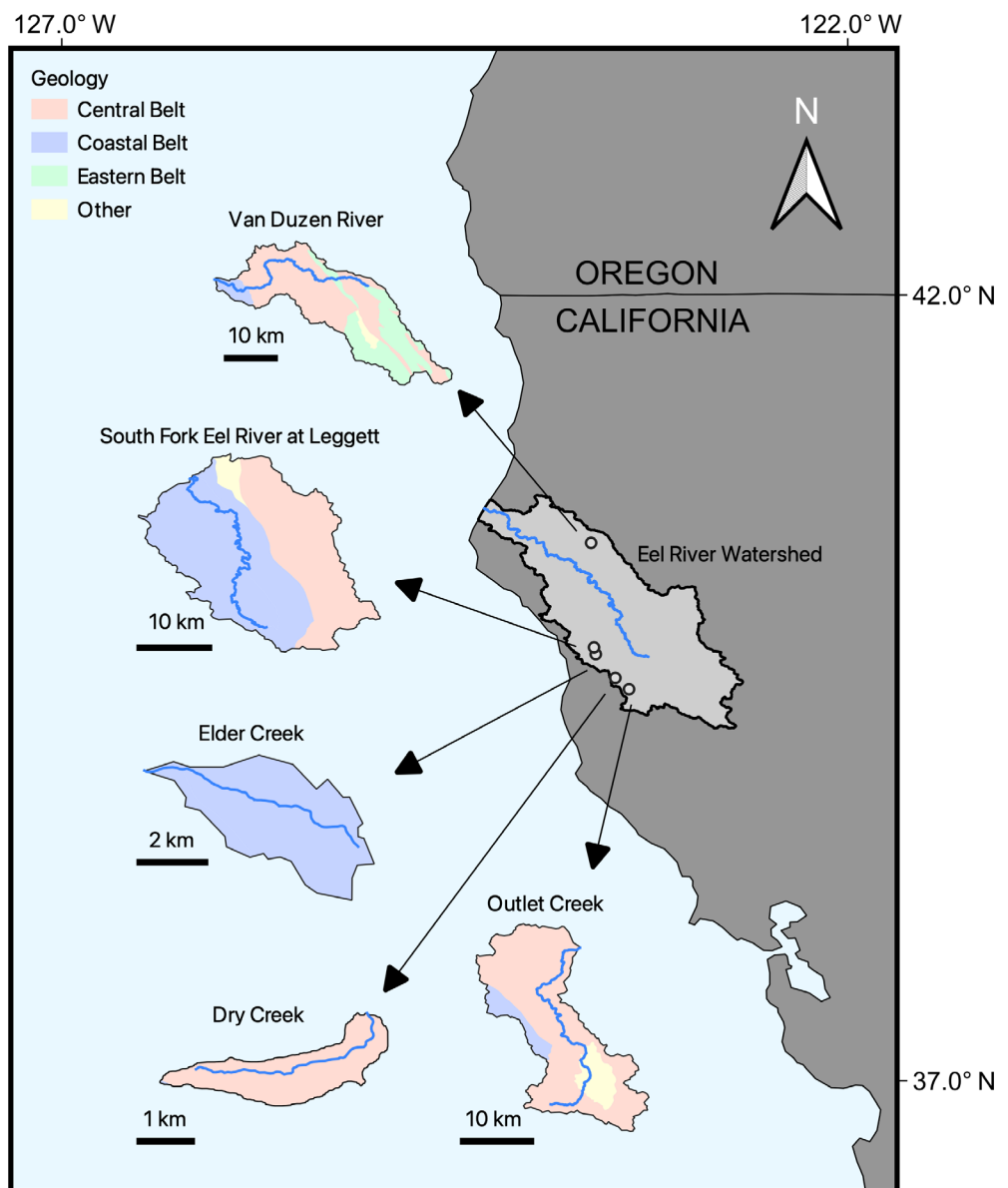
## GEOLOGY, SUBSURFACE STRUCTURE, AND STORAGE

The study area encompasses multiple sub-watersheds (Table 2 and Figure 1) of the Eel River in the Northern California Coast Ranges. The regional climate is Mediterranean type with warm, dry summers and cool, wet winters (most precipitation arrives between November and April). The Eel River basin is underlain by the Franciscan Complex, a geological assemblage in Northern California consisting of three north-south running belts (the Coastal Belt, the Central Belt melange, and the Eastern Belt) of different rock types that decrease in age and metamorphic grade from east to west (Dott & Shaver, 1974; McLaughlin et al., 1994).

**TABLE 2** Environmental characteristics of the studies' watersheds.

Watershed	USGS gage ID	Area (km <sup>2</sup> )	Elevation range (m)	Mean annual precipitation (mm)	Mapped % melange geology <sup>a</sup>
Dry Creek	N/A	3.5	605–885	1776	100%
Outlet Creek	11472200	418	319–1043	1476	82%
Van Duzen River	11478500	574	113–780	1789	62%
Eel River, Leggett	11475800	642	211–1280	1927	41%
Elder Creek, Branscomb	11475560	16.8	440–1277	2309	0%

<sup>a</sup>Nonmelange geology for these watersheds is predominantly Coastal Belt, with the exception of the Van Duzen River, which includes approximately 30% Eastern Belt. Annual rainfall data are derived from the PRISM Climate Group (PRISM Climate Group, 2004) daily rainfall product found on the Google Earth Engine Data Catalog from 1981 to 2020.

**FIGURE 1** Overview map of the study watersheds. Points in the main map are located at each watershed's centroid. Coastal, Central, and Eastern Belt geologies are mapped in light blue, light red, and light green, respectively, in inset maps.

Two intensively monitored watersheds within the Eel River basin, Elder Creek and Dry Creek, serve as representative end-members of the Coastal Belt (Elder Creek) and Central Belt melange (Dry Creek). Figure 2 illustrates lithologically determined contrasts in hillslope subsurface structure—and thus water storage capacity—in the two watersheds. We here provide a brief overview of the subsurface structures and water storage dynamics at these two end-member sites. These descriptions are later used to explain the hydrological behavior of larger watersheds that contain both geologies. For more details on Dry Creek and Elder Creek, we refer the reader to Hahm, Rempe, et al. (2019).

Dry Creek is underlain by the Central Belt melange geology (Figure 2 left column), a chaotic mixture of bedrock of varying lithology and size suspended in a shale-derived, clay-rich matrix that is perennially saturated in the underlying fresh bedrock, which lies just 2–3 m

below the ground surface. The thin weathering zone of the Central Belt completely fills to saturation after approximately 200 mm of wet-season rainfall, at which point the groundwater table rises to the surface, generating widespread saturation overland flow that is rapidly routed to dense drainage networks. Consequently, the Central Belt watersheds are unable to store large volumes of wet-season precipitation, resulting in fast draining hillslopes, and streams that cease flowing within the first couple of months of the dry season (Lovill et al., 2018). Low storage also results in a more water-stress-tolerant savanna plant community comprised primarily of Oregon white oak (*Quercus garryana*) and annual grasses (Hahm et al., 2018). The watershed is very lightly grazed seasonally, but satellite records show that long-standing fence lines do not result in major differences in plant biomass or biome type (see video in Hahm, Rempe, et al., 2019). No salmonids have been observed in Dry Creek, likely due to a steep

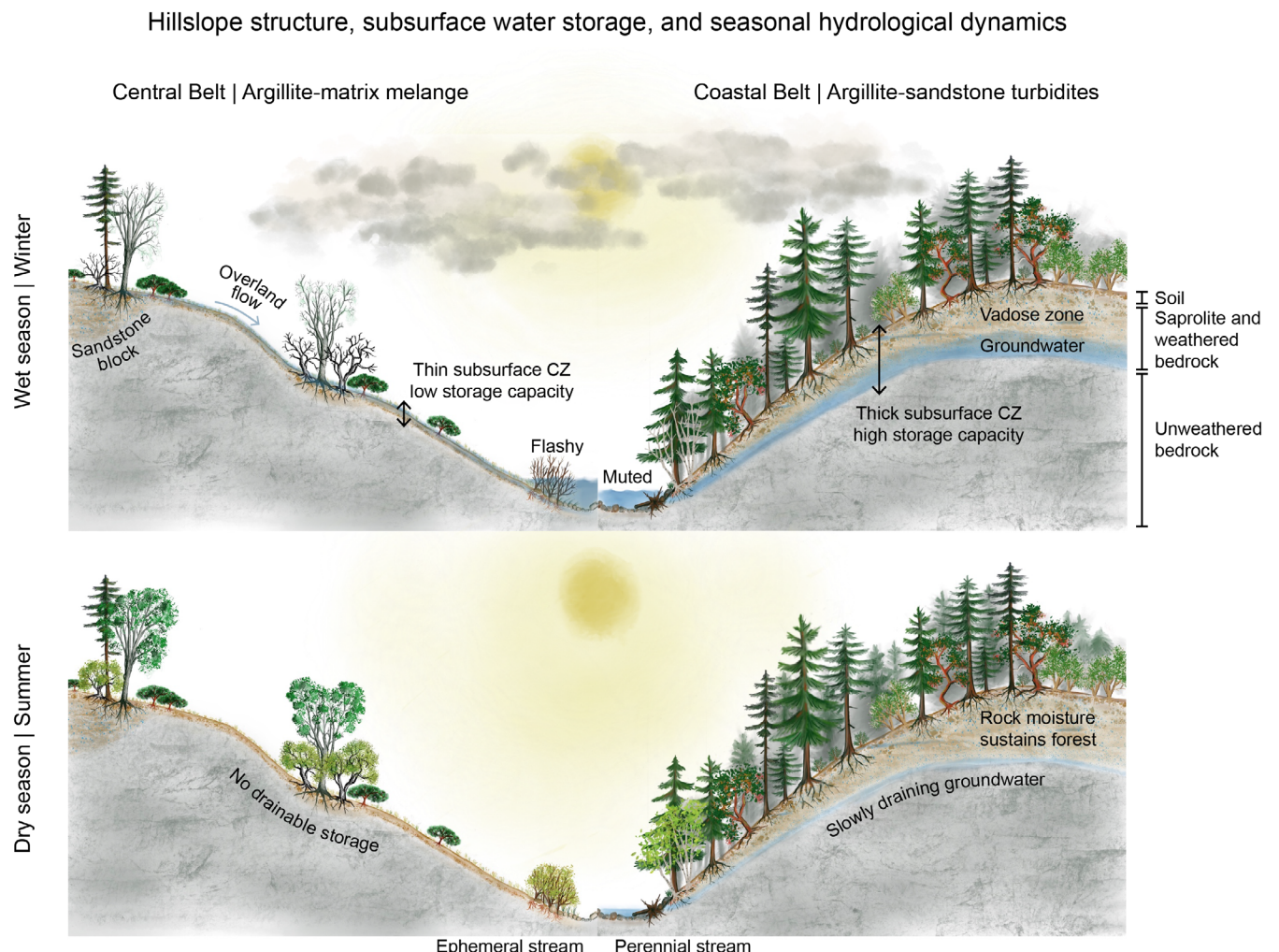


**FIGURE 2** Seasonal hydrological dynamics between hillslopes representing two dominant geologies in the Eel River watershed—Central Belt melange (left) and Coastal Belt turbidites (right)—leading to contrasting critical zone (CZ) architectures and water storage capacities. A typical wet-season (winter) snapshot is depicted in the top row, while the bottom row illustrates conditions later in the dry season (summer).

megaboulder-pinned knickpoint (e.g., Roering et al., 2015) just downstream of the Dry Creek outlet. Salmonids are nevertheless commonly found in other small melange streams (e.g., Rossi et al., 2022) and throughout the Eel River watershed, which integrates flow and temperature signals from both Central and Coastal Belt streams.

The Elder Creek watershed is underlain by the fractured shale and sandstones of the Coastal Belt (Figure 2 right column). Deep weathering profiles (upwards of 30 m at hilltops, thinning toward the channel) in the Coastal Belt have resulted in large water storage capacity of the subsurface, most of which is unsaturated storage (Dralle et al., 2018) in a thick vadose zone that includes soil, saprolite, and weathered bedrock. This unsaturated reservoir can hold upwards of 300 mm of seasonally dynamic water storage, equal to more than one third of annual wet-season precipitation during dry years (Rempe & Dietrich, 2018). The large dynamic storage in the vadose zone is the primary water source for the productive, dense conifer-hardwood evergreen forests found in the Coastal Belt. Despite decades of logging throughout the Coastal Belt (though not Elder Creek), plant assemblages remain the same (Hahm, Rempe, et al., 2019). Historically, Native American burning expanded the area of dominant hardwoods relatively to conifer, but with suppression of fires, conifers are actively invading and replacing these areas (e.g., Cocking et al., 2012). Following the long dry season, tree-driven storage deficits (the amount of water input to the root zone required to replenish that which vegetation removed) in the unsaturated zone are typically replenished within the first few months of the wet season (October–December), whereupon the soil and weathered bedrock layers wet to a characteristic maximum storage. Analogously to “field capacity” in soils (Grindley, 1968), additional rainfall beyond this characteristic maximum value triggers gravitational drainage that recharges an underlying fractured-rock hillslope groundwater system, which flows laterally downslope, discharging to streams through a system of seeps and springs (Lovill et al., 2018; Salve et al., 2012). This deeper saturated reservoir can store upwards of 200 mm of dynamic, drainable groundwater (in addition to the 300 mm of dynamic storage in the unsaturated soils and rock) that supports year-round cold baseflows.

## WATER STORAGE DYNAMICS AND RUNOFF

Using hydrological and climatic data from the Dry and Elder Creek end-members, we explore storage capacity controls on flow regime features that matter for fish: timing of wet-season flow activation (I), peakflow magnitude (II), flow recession rate (III), and low flow

magnitude (IV) (Yarnell et al., 2020). Figure 3 provides an overview of contrasting flow regime features in the end-member Coastal and Central Belt watersheds. Center panels plot discharge on linear (top central panel) and log (middle central panel) scales, as well as cumulative discharge and runoff, for the 2019 water year. The paneled subplots aim to highlight the major functional flow components I–IV. Importantly, the sites’ 20-km separation results in nearly identical rainstorm magnitudes through the winter.

Conceptual figures illustrate many of these outcomes. A four-quadrant hillslope diagram (Figure 2) depicts representative hydrology for the two end-member geologies in both the wet and dry seasons, and a four-quadrant stream diagram (Figure 4) depicts the typical trajectory of stream conditions from the spring/early summer flow recession to the late summer low flow period.

## Wet-season flow activation

Differences in vegetation cover between Elder and Dry (left vs. right column in Figure 2) result in different magnitudes of plant water use, and thus differences in storage deficits in the root zone at the end of the dry season (Dralle et al., 2018; McCormick et al., 2021; Wang-Erlandsson et al., 2016). Replenishment of these deficits via infiltration of rainfall and filling of the CZ at the start of the wet season mediates drainage from the root zone, thereby determining the amount of rainfall (more at Elder) required to recharge the hillslope aquifers that drive streamflow production (either via subsurface flow or groundwater-driven saturation overland flow) at the hillslope–channel boundary (Dralle et al., 2018; Grindley, 1968; Lapides et al., 2021; Müller et al., 2014).

To quantify storage controls on wet-season flow activation, we turn to a storage-activation approach introduced by Sayama et al. (2011), wherein early wet-season discharge is plotted as a function of cumulative seasonal dynamic watershed storage to identify storage thresholds that lead to rapid increases in discharge. Figure 3I plots daily stream discharge for the initial wet-season months (October through December 2018) against a catchment water storage approximation, calculated as the running sum of input (precipitation,  $P$ ) minus output (discharge,  $Q$ ) fluxes beginning on October 1, under the assumption that differences between these two dominant fluxes can be attributed to the accumulation of storage in the watershed (approximation of Equation 1,  $\Delta S = P - Q - ET \approx P - Q$ ). Evapotranspiration is neglected because it is expected to be relatively small given the lower temperatures and more cloudy conditions during October–December when

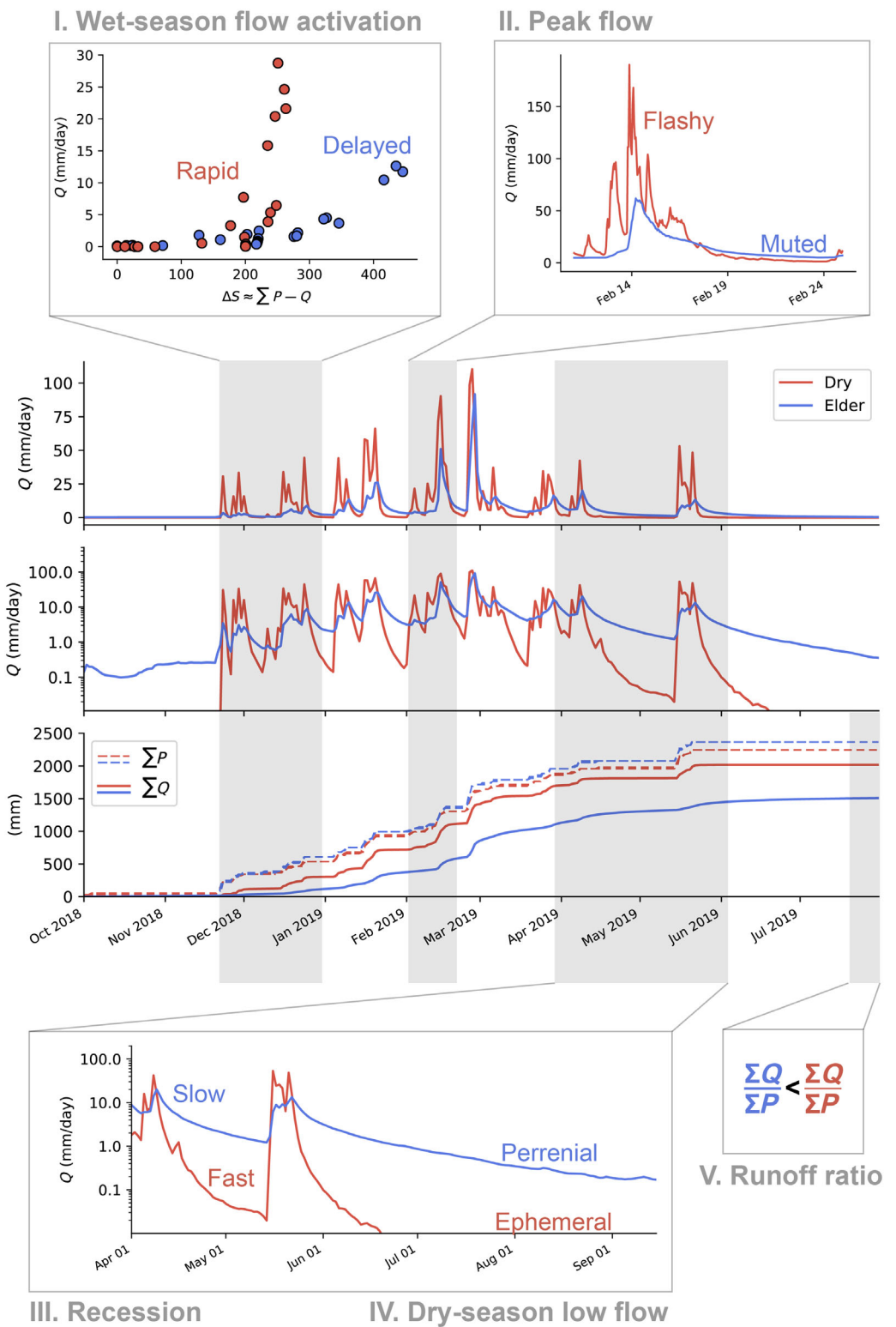


**FIGURE 3** Storage capacity impacts important flow regime characteristics. Roman numerals correspond to entries in Table 3, while blue and red colors correspond to the Elder Creek and Dry Creek watersheds, which are representative end-members of the Coastal Belt (relatively high storage capacity) and melange (low storage capacity) geologies, respectively. The top two subplots of the center panel show 2019 water year hydrographs (on linear and log scales), while the bottom subplot shows cumulative precipitation ( $\sum P$ ) and cumulative discharge ( $\sum Q$ ). Focus panel (I) plots initial wet-season daily discharge values through December 2018 as a function of the approximate dynamic storage  $\sum P - Q$ . (II) Shows an expanded view of peak flows during a typical wet-season storm sequence after initial set-up. (III) Illustrates differences in recession rates, while (IV) demonstrates how recession rate determines whether streams continue to flow through the entire dry season. (V) Shows that a greater fraction of precipitation is converted to runoff in the Dry Creek watershed.

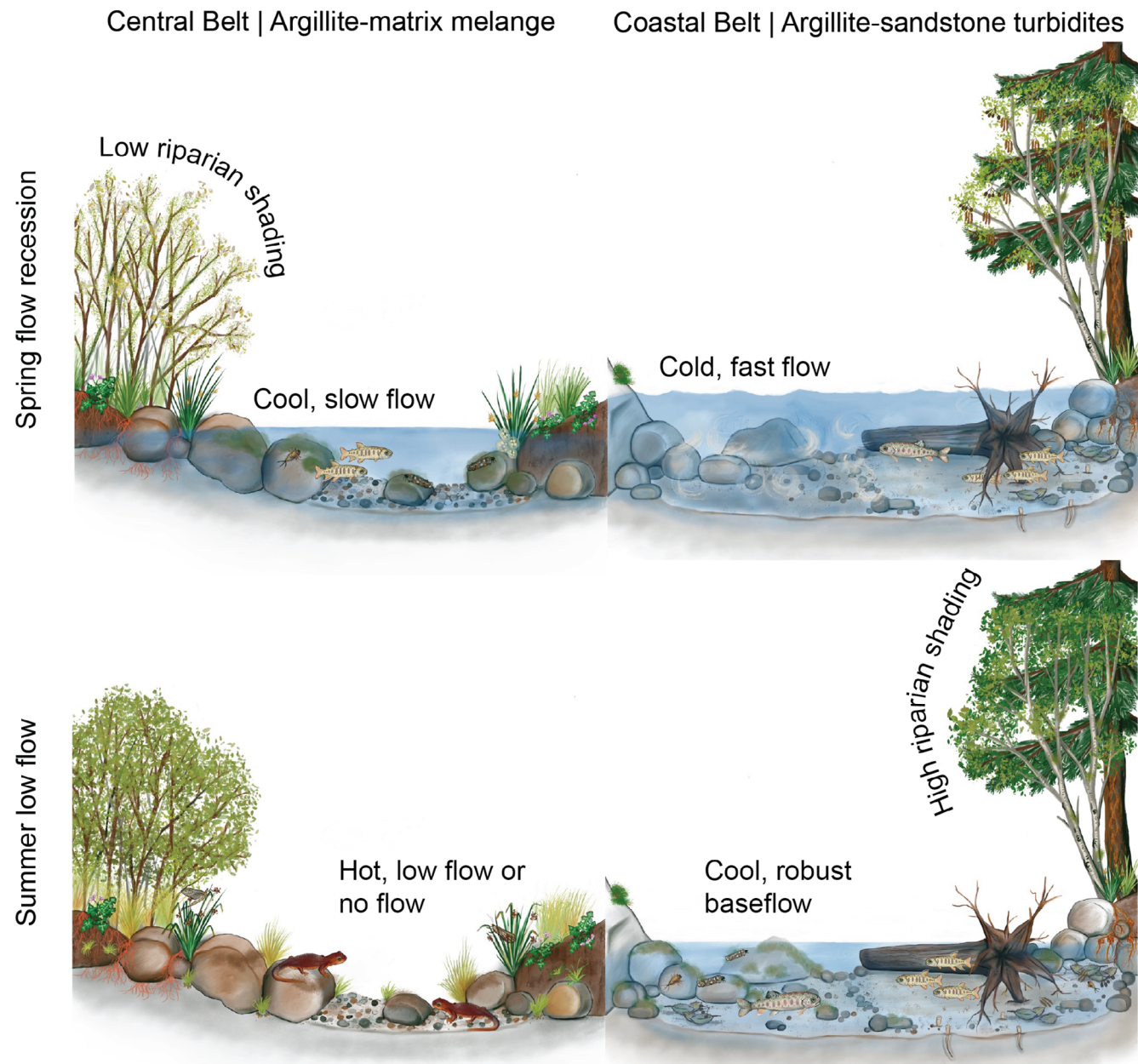


**FIGURE 4** Typical progression of stream conditions between the Central Belt melange (left) and Coastal Belt turbidites (right) following the last significant rainfall event of the wet season. The top row illustrates conditions in the spring/early summer when air temperatures have begun to increase and streamflow is beginning its long seasonal recession. The bottom row depicts late summer low flow conditions when air temperatures are high and water availability in the stream is approaching its annual minimum.

the sum is calculated. Flow activation in Dry Creek begins around approximately 150 mm of cumulative rainfall at the start of the wet season, whereas Elder Creek flow does not activate until approximately 300 mm of rain has fallen. Moreover, Elder Creek discharge sensitivity to storage is much lower, as can be seen by the relatively muted increase in discharge with storage increases beyond 300 mm. The storage–discharge relationship in Dry Creek is more nonlinear (“flashier”), with a very steep increase in flow rate beyond 200 mm of storage.

## Peak flow magnitude

The relationship between storage and discharge also explains the difference in peak flow magnitudes in Figure 3II, where the smaller storage capacity at Dry Creek results in more extreme peak flows. Very small changes in storage generated by the addition of precipitation result in rapid, highly nonlinear increases in flow at Dry Creek and correspondingly large peak flows, which contrast Elder Creek’s muted peak flow response during

rainfall events. These flow behaviors can be attributed to water storage dynamics in the hillslope, where complete filling of the CZ in the Central Belt results in flashy streams fed predominantly by saturation overland flow, as compared with the muted groundwater-dominated signal in Elder Creek, as illustrated in Figure 3.

## Rate of recession and low (base)flow magnitude

Whereas Figure 3I and II shows the effect of storage capacity on the rising limb and peak flow behaviors, Figure 3III and IV demonstrates that storage capacity is also a strong determinant of the drainage behavior of the study catchments. At Dry Creek, small storage capacity drives water to the surface, where shallow and overland flow paths result in fast flow recessions and very little retention of drainable storage. In the Elder Creek watershed, the drainage of deeper fractured-rock hillslope groundwater results in a much slower recession and high retention of drainable groundwater storage going into the dry season. The consequences of these recession dynamics are illustrated in the top row of Figure 4. The rapid drop in flows in Central Belt catchments results in relatively mild flow conditions during a short period in the spring (see much of April and May in Figure 3), which contrasts the persistently higher flows during the early dry season in Coastal Belt watersheds.

Over longer periods of drainage—California's protracted dry season can persist for more than six months of the year—storage capacity may dictate whether a stream has any water at all. In our study catchments, two distinct dry-season flow regimes emerge: high storage capacity Elder Creek supports robust baseflows that persist through the dry season, whereas ephemeral flows in Dry Creek result in dry streambeds typically before July (Figure 4).

Interestingly, although there is lower dry-season baseflow in the Dry Creek watershed, over the course of an entire year, Dry Creek typically generates more total runoff for a given precipitation event, as quantified by each watershed's runoff ratio in 3V. From water year 2016 through water year 2020, the average runoff ratio in Elder Creek is approximately 0.6, compared with an average runoff ratio of approximately 0.8 at Dry Creek. The small storage capacity at Dry Creek generates enough runoff during the wet season to overwhelm its small dry-season runoff totals, thus producing an overall higher runoff ratio. We attribute this difference primarily to the significant amounts of water stored in the thick weathered bedrock vadose zone at Elder Creek, which results in more water being returned to the atmosphere via transpiration during the growing season.

## Spatial and temporal variability in water availability

In addition to impacting average flow regime features “at a station,” storage capacity can also mediate the spatial availability of water via the wetted channel network and the sensitivity of runoff dynamics to year-to-year swings in rainfall totals. For example, Lovill et al. (2018) demonstrate significant differences in wetted channel drainage density (the total length of wetted channels in a catchment divided by the area of that catchment) between the Elder Creek and Dry Creek watersheds. Figure 5 reproduces results from Lovill et al. (2018), plotting a snapshot of wetted channel extent in late August 2014. On this date, Elder Creek wetted channel drainage density is nearly 10 times greater than that observed in Dry Creek, despite nearly identical rainfall totals in the preceding wet season.

### VI. Dry season wetted channel extent

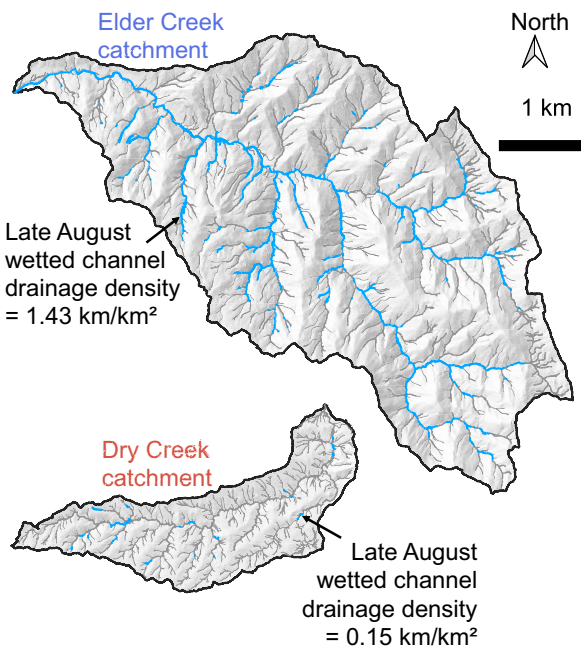


**FIGURE 5** Dry-season wetted channel extent is approximately 10-fold higher in the representative Coastal Belt watershed (Elder Creek) than in the representative Central Belt watershed (Dry Creek). Cyan lines denote liquid water at surface in channels (including all stagnant pools and flowing reaches, whether disconnected or continuous). Light gray lines denote approximate geomorphic channel extent. Each catchment is shown to scale, but their relative locations have been modified for display purposes. Wetted channel data from Lovill et al. (2018); Elder Creek surveyed in 2014, Dry Creek in 2015 (rainfall was similar between the sites for these different years; PRISM-derived precipitation was 1160 mm in Elder Creek in 2014, and 1290 mm in Dry Creek in 2015 (PRISM Climate Group, 2004). Light detection and ranging-derived hillshade underlays from data collected by NCALM (Dietrich, 2014).

Hahm, Dralle, et al. (2019) introduce the idea that small subsurface water storage capacity relative has the potential to decouple end-of-wet-season storage (which sets plant water availability during the dry growing season) from total annual rainfall. This mechanism was dubbed “storage capacity limitation,” where because subsurface storage capacity is small relative to mean annual precipitation, storage fills to that capacity in both wet and dry years, resulting in a decoupling between water storage and annual rainfall totals (Figure 6). On the other hand, Hahm, Dralle, et al. (2019) identified “precipitation-limited” sites as places where the catchment storage capacity is larger than the average annual precipitation. Large storage capacity catchments will not fill to capacity in wet or dry years, and thus storage will be more strongly coupled to annual swings in precipitation totals.

Although Hahm, Dralle, et al. (2019) explore this concept with respect to vegetation response to annual rainfall variability, it may extend to components of hydrograph variability as well. Specifically, since storage controls summer low flows (Dralle et al., 2016), decoupling storage from annual rainfall (as seen in storage-capacity-limited locations) will lead to decoupling of low flows from annual rainfall. In both Elder Creek and Dry Creek, we find that dry-season low flows are decoupled from annual swings in total rainfall. This is because storage capacity in both

watersheds is significantly lower than average annual precipitation, and therefore annual variations in total rainfall do not lead to annual variations in storage going into the dry season. Importantly, the storage capacity limitation argument does not necessarily lead to an absolute prediction of low flow magnitude; instead, the mechanism modulates the sensitivity of low flow magnitudes to annual precipitation.

In the case of Dry Creek, this decoupling result is trivial; low flows are reliably zero in all years, and therefore low flow magnitudes are insensitive to swings in total annual rainfall. Although not plotted, for the four water years (2016–2019) with complete data at Dry Creek, zero-flow duration (number of dry-season days during which flows are zero; a low flow metric for ephemeral streams) exhibits no correlation with annual total precipitation ( $R^2 = 0.21$ ). At Elder Creek, parallel recession curves across all years in Figure 7a suggest that dry-season initial flow conditions/timing and dry-season duration (both set by shoulder season rainfall patterns) are likely more important than total rainfall as a driver of low flow magnitude. Figure 7b quantifies the decoupling between low flow and annual rainfall, demonstrating that low flow magnitude (over 21 years, 2001–2021) does not vary strongly with total rainfall. Consistent with the storage capacity limitation mechanism hypothesized by Hahm, Dralle,

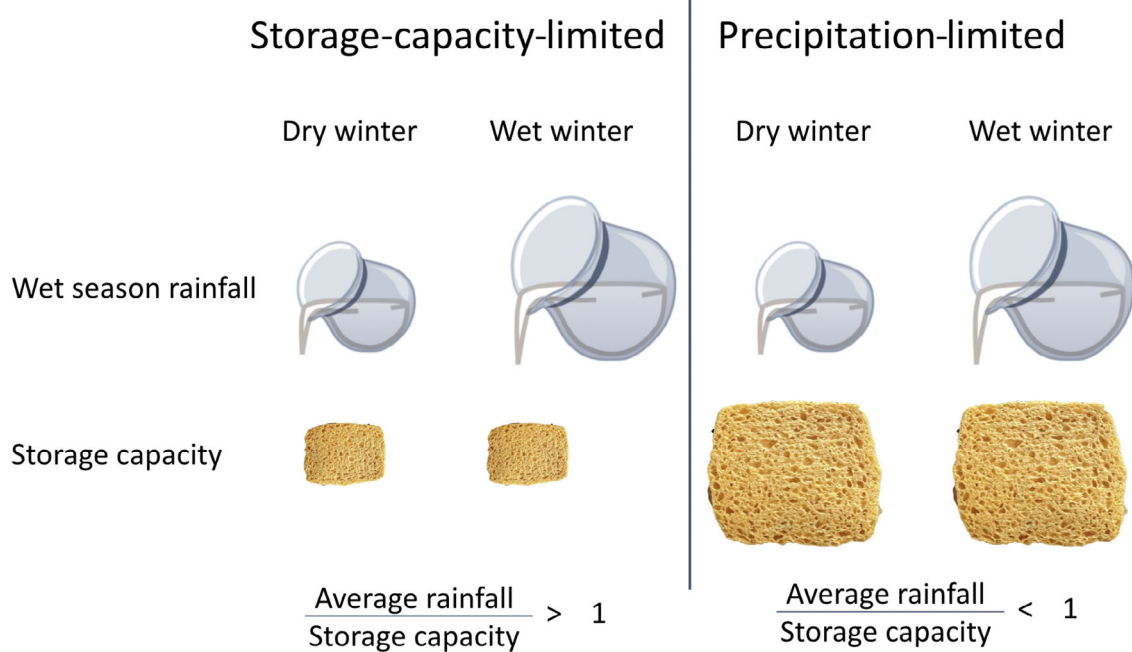


**FIGURE 6** Simplified conceptual cartoon of the storage capacity limitation mechanism (hydrological model described fully in Hahm, Dralle, et al., 2019). In catchments where storage capacity (the size of the sponge) is small relative to mean annual precipitation, the sponge will fill to capacity in relatively wet and dry years, resulting in a decoupling between storage and total precipitation (i.e., more precipitation does not result in more storage). Conversely, in precipitation-limited locations (right), the sponge is large relative to mean annual precipitation. Therefore, in wet years, the large sponge has the capacity to store more, and in dry years, it will store less, resulting in a stronger coupling between storage and annual precipitation.

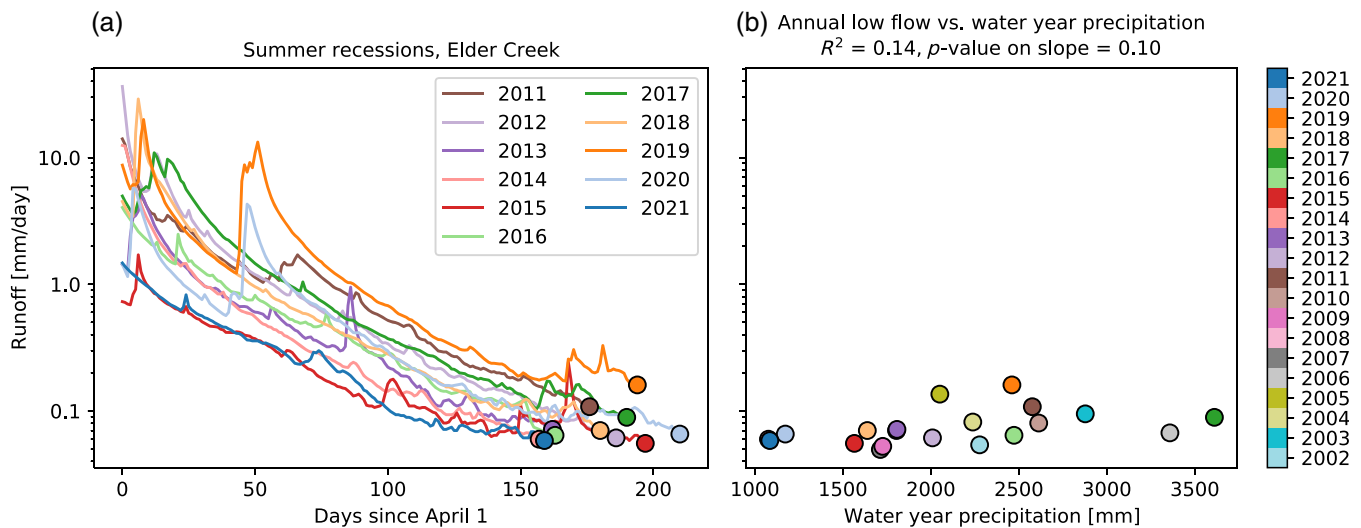


**FIGURE 7** Storage capacity decouples annual low flows from total water year precipitation at Elder Creek. (a) Plots summer recessions as a function of days after April 1 from 2011 water year through 2021 water year, stopping on the day with the lowest observed flow for that calendar year (through December). The second subplot (b) shows that annual total precipitation is not a strong predictor of dry-season low flows due to the mechanism of storage capacity limitation. End-of-dry-season low flow conditions are more strongly controlled by rainfall conditions during the transition between wet and dry seasons. Annual rainfall data are derived from the PRISM Climate Group (PRISM Climate Group, 2004) daily rainfall product found on the Google Earth Engine Data Catalog.

et al. (2019), a linear regression reveals no significant slope on the low flow versus water year precipitation relationship, with an  $R^2$  of 0.14, indicating that water year precipitation explains little of the variation in summer low flows.

## Hydrological scaling in mixed-lithology watersheds

Large watersheds can be conceived of as a collection of hillslopes connected through a shared channel network (e.g., Harman et al., 2009). Using this unit-hillslope concept, and under the assumption that a map of Coastal and Central Belt geologies may serve as a proxy for hillslope storage capacity across the Eel River, we hypothesize that mixed-lithology watersheds will behave, hydrologically, like a superposition of the Elder Creek and Dry Creek geological end-members. To test this hypothesis, we identified five sub-watersheds (Table 2) of the Eel River with contributing areas less than  $1000 \text{ km}^2$  that span a gradient in percent melange composition, where Dry Creek serves as the 100% melange watershed and Elder Creek serves as the 0% melange watershed. We explore scaling of flow recession and dry-season water availability across this geological spectrum of sites.

We perform two analyses to explore drivers of the scaling of dry-season flow recession (e.g., Figure 8a) and water availability in the watersheds listed in Table 2. First, we calculated a dimensionless metric of

summer water availability, the summer runoff fraction, which is calculated as the long-term average of the annual ratio of total flow from June through September (summer dry season) divided by total flow from the previous October through May (preceding wet season). Second, we calculated the average flow recession rate using the widely used exponential flow recession model:

$$\frac{dQ}{dt} = -\frac{1}{\tau} Q \rightarrow Q = Q_0 e^{-t/\tau},$$

where  $Q_0$  is the initial flow value at the start of the recession. The recession timescale,  $\tau$  (with units of time), is a scale-independent measure of the rate of recession and is therefore directly comparable between watersheds of different sizes and with different average flow values.

Watersheds with a greater percent of Central Belt melange contributing area have less summer runoff relative to annual total runoff (Figure 8b). At Elder Creek (0% melange), we see an average of 3.75% of annual runoff discharges during the summer months. There is a monotonic decrease in summer runoff fraction, with effectively 0% of annual runoff occurring during the summer months in Dry Creek (100% melange).

Figure 8a,c explains why summer runoff fractions are so small in melange-dominated watersheds: typical flow recession rates, as quantified by the linear recession timescale ( $\tau$ ), decrease nearly 10-fold across the geological gradient, from approximately  $\tau = 10$  days at Elder Creek

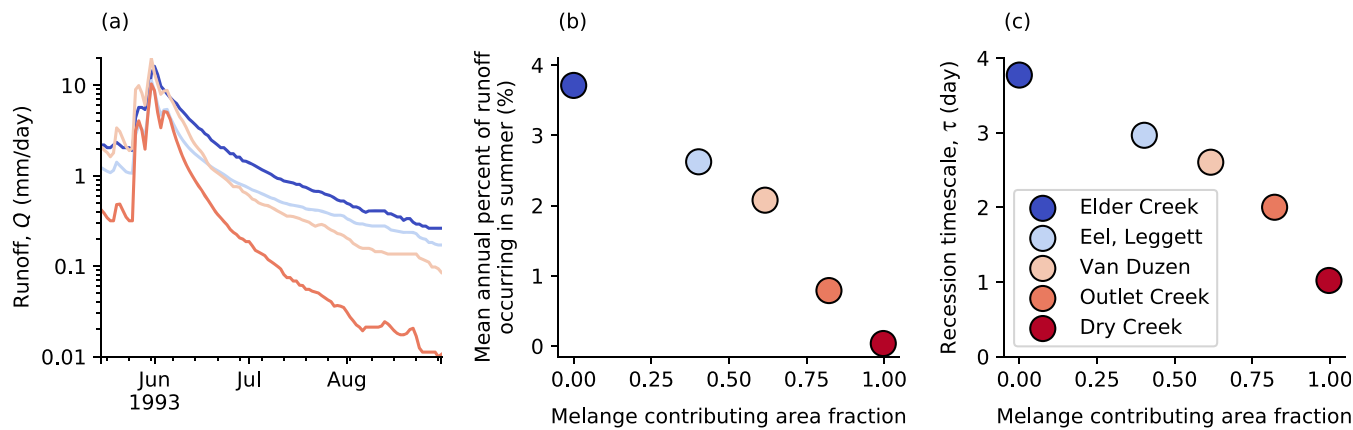


**FIGURE 8** Watersheds across a gradient in fraction of melange contributing area illustrate a range of flow recession behaviors (a). The five colored points refer to the watersheds described in Table 2. Faster flow recessions in melange watersheds decrease water availability during the dry season, as demonstrated by the decrease in summer runoff fraction with increasing melange fraction (b). Conversely, Coastal Belt watersheds drain much more slowly, resulting in perennial flows and robust dry-season discharge. Recession analysis (c) shows that larger fractional melange contributing area results in faster recessions, as quantified by a simple exponential recession model:  $Q(t) = Q_0 e^{-t/\tau}$ . Smaller values of  $\tau$  in melange-dominated watersheds correspond to faster recessions (i.e., rapid timescales of drainage).

to  $\tau=1$  day at Dry Creek. Actual recession data in Figure 8a illustrate how smaller recession  $\tau$  results in a more rapid drop in flows in watersheds with higher melange fraction.

## ENERGY BUDGETS AND STREAM TEMPERATURE

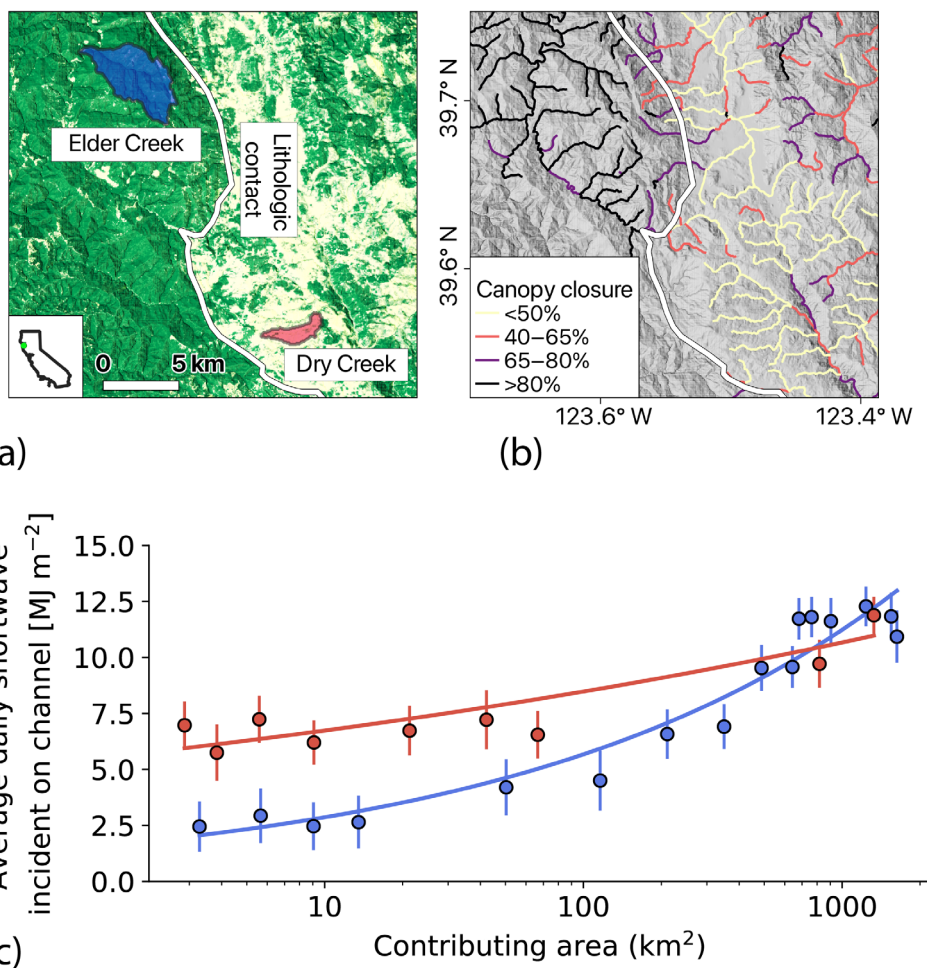
Figure 9 illustrates radiation and temperature dynamics relevant to energy budgets in stream channels, and thus factor in the consideration of stream water temperature and light environment. Different subsurface water storage capacities support distinct vegetation types: dense, shady forest at Elder Creek, and at Dry Creek, a deciduous oak savanna admitting more solar radiation (Figure 4). Differences in runoff pathways and flow volumes between the Elder Creek and Dry Creek watersheds should also affect stream temperature and its sensitivity to changes in atmospheric conditions. Deeper groundwater flow paths in Coastal Belt geologies (Figure 2) are more buffered from variations in air temperature (which can impact hillslope throughflow temperatures [Leach & Moore, 2015]) or solar radiation. The thermal inertia of a stream can also be expected to vary with flow volumes; all else equal, stream temperature will be more responsive to changing atmospheric conditions at smaller flow volumes. For all these reasons, stream temperature in watersheds with lower storage capacity, like Dry Creek, should more closely track changes in air temperature, which drives many components of the channel energy budget via the Stefan–Boltzmann law, and often

correlates with shortwave solar radiation delivery (Westhoff et al., 2007).

## Channel shading

Large differences in canopy cover between the two geologies can be seen in Figure 9a. These storage-driven differences in vegetation community and canopy cover affect the riparian light environment. To quantify this, we calculated a simplified light penetration index (LPI) metric (Bode et al., 2014) as the number of light detection and ranging (LiDAR) point returns that strike either ground or water divided by the total number of LiDAR returns at a 1-m resolution across all available LiDAR datasets in the Eel River (Dietrich, 2014, 2015; Perkins, 2009; Power, 2013; Roering, 2006). The LPI estimates the fraction of shortwave radiation that penetrates the vegetation canopy to reach the ground or water surface. Using mapped LPI, we computed reach-averaged canopy closure (Figure 9b) throughout the Eel River basin, illustrating a significant shift in stream shading across the Coastal and Central Belt lithologic contact. We then explored how this shift in riparian cover impacts the growing season stream energy budget by first extracting total summer shortwave solar radiation delivery (June through August) from the midpoint (latitude 39.64, longitude -123.53) of the centroids of the Elder and Dry Creek watersheds (Thornton et al., 2020), and then multiplying this figure by reach-averaged LPI to arrive at an estimate of total shortwave solar energy delivery to streams over the peak growing season months.

## VII. Channel shading



## VIII. Stream temperature

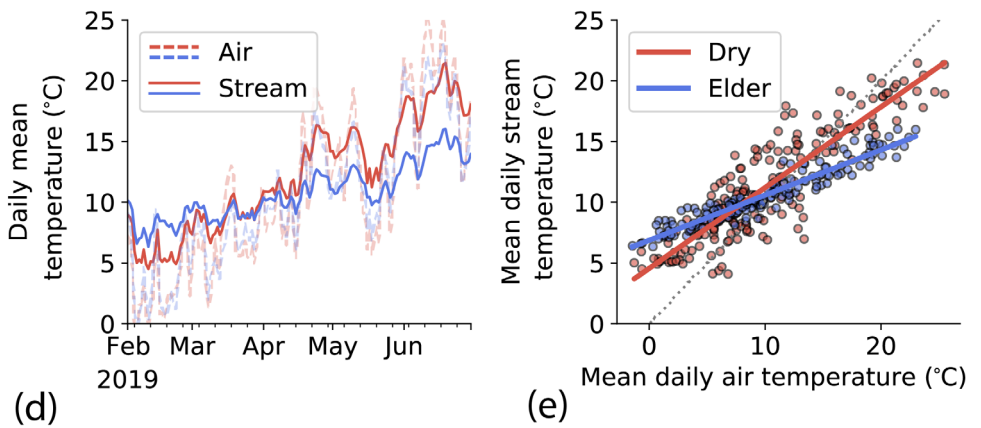


**FIGURE 9** Differences in storage capacity across the geologic contact lead to stark differences in vegetation cover (a). Representative end-member catchments are outlined. Differences in canopy cover result in smaller delivery of shortwave radiation to headwater channel surfaces during summer months (June, July, and August) in the Coastal Belt (west of contact) versus Central Belt (east of contact) (b). With increasing contributing area, channels widen, resulting in a convergence of channel-incident shortwave radiation between the two geologies (c). Red and blue points are binned averages  $\pm$  one standard deviation, from all Central Belt and Coastal Belt channels, respectively, in the study area with available light detection and ranging data. Bin spacing varies to ensure a sufficient number of samples in each bin according to the procedure described in Kirchner (2009). We hypothesize that contrasting stream temperature dynamics (d) are due to differences in flow pathways, flow volumes, and riparian light environment. Subplot (e) demonstrates significantly higher sensitivity to changes in air temperature in the Dry Creek watershed.

Figure 9c plots the reach-scale, LPI-filtered solar shortwave radiation energy delivery across a range of watershed contributing areas for the two lithologies. At small contributing areas, solar energy delivery to the channel is nearly three times greater in Central Belt versus Coastal Belt watersheds. However, as contributing area increases, channel widths tend to increase, leading to an overall increase in solar radiation delivery and a convergence between the two lithologies: streamside vegetation shading matters less in wide channels.

## Stream temperature

Figure 9d plots air temperature and stream temperature at the end-member sites, clearly demonstrating that Dry Creek water temperatures fluctuate more widely than those in Elder Creek despite nearly identical air temperatures between the two sites. Figure 9e removes the time element to reveal the relationship between water temperature and air temperature. Best fit lines between Elder Creek and Dry Creek show that water temperature is generally buffered relative to air temperature as expected from its higher heat capacity (slope less than 1) but that Dry Creek's best fit line slope is nearly double that of Elder Creek, indicating that Dry Creek water temperature is much more sensitive to atmospheric conditions.

## SALMONIDS AND THE SUBSURFACE—LIFE HISTORY FRAMEWORK AND HYPOTHESES

### Life cycle of anadromous Pacific salmon in the Eel River

The Eel River is home to at least five distinct runs of Pacific salmon: fall-run Chinook salmon, coho salmon, winter and summer steelhead, and coastal cutthroat trout (Yoshiyama & Moyle, 2010). The majority of these animals exhibit an anadromous life history in which adult fish spend 2–5 years in the ocean before returning to spawn in the river. The timing of river entry and spawning varies between and within species and between water years and spawning sites. Typically, in the Eel River Chinook spawn first (October–February), followed by coho (November–March), and lastly steelhead (December–April). After spawning, the fertilized eggs incubate in gravel nests called “redds” for 1.5–4 months before hatching as larva called “alevins” with attached yolk sacs (National Marine Fisheries Service, 2014). Alevins continue to live in or near the redd as they absorb their yolk sacs at which point they are called fry. Fry typically inhabit stream margins and

shallow water and begin feeding on small stream insects. However, fry often maintain close proximity to their redds for up to 10 weeks (National Marine Fisheries Service, 2014). Fry may distribute throughout the river system or rear in tributaries as they develop into “parr” (typically 60–100 mm long). Parr may live in the river system between 3 months and 3 years before they begin migrating to the ocean. Prior to entering saltwater, parr undergo a complex behavioral, developmental, and physiological transformation known as “smoltification” (McCormick et al., 2013). Smoltification allows juvenile salmon to develop seawater tolerance by altering their major osmoregulatory organs, primarily the gills, gut, and kidney (McCormick et al., 2013). Finally, “smolts” (or pre-smolts) enter the estuary where they may rear for days to months before ultimately entering the ocean. While this general description outlines the major freshwater life stages of Pacific salmon in the Eel River, there is tremendous life history diversity among the Eel River's juvenile salmon both within and between species. This life history diversity is driven by genetics and also emerges from the different environmental conditions, including physical (e.g., flow and temperature) and biotic (e.g., food web–species interactions) regimes that salmon and trout encounter during their freshwater residency.

### Life history syndromes

Properties of the subsurface CZ have consequences for salmonids across every stage of their life history. Environmental regimes determined by a watershed's storage capacity in turn constrain (Table 3) opportunities for salmon, influencing access for migrating and spawning adults, the incubation and survival of eggs, and the rearing habitats and movements of juveniles during their freshwater residence. A particularly diverse component of the many life histories of anadromous salmonids (Hodge et al., 2016; Shapovalov & Taft, 1954) is residence time of juveniles in their natal streams and their corresponding dependence, or lack thereof, on rearing outside their natal habitats. Here we suggest that watersheds with different and distinct subsurface storage capacities will favor the emergence of life history syndromes, that is, suites of correlated traits associated with different degrees of dependence on natal and non-natal rearing (Buoro & Carlson, 2014).

In nonperennial systems such as Dry Creek, faster recession that lowers summer baseflow should favor a “grow fast and out-migrate early in life” strategy (e.g., Erman & Leidy, 1975), while earlier flow activation will allow adults to access and spawn sooner than in perennial streams (Figure 3). Warmer water would also

**TABLE 3** Observed impacts of hillslope subsurface water storage capacity on streamflow characteristics in rain-dominated, Mediterranean climates.

Category	Metric	Relative impact	Hypothesized reason/mechanism
Water	I. Wet-season flow activation	Later with bigger storage capacity	More rain required to replenish bigger dry-season hillslope water storage deficits
	II. Peakflow magnitude	Higher with smaller storage capacity	Small storage capacity more likely to fill, prompting greater and activation of faster (shallow near surface or overland) runoff pathways
	III. Rate of recession	Higher with smaller storage capacity	Deep slow flow paths versus shallow fast flow paths
	IV. Mean low (base)flow magnitude	Higher with bigger storage capacity	Greater reservoir to sustain dry-season flow
	V. Annual runoff ratio	Lower with bigger storage capacity	More rainfall is partitioned to evapotranspiration where storage capacity is greater, enabling storage of wet-season rainfall for dry-season use by plants
	VI. Dry-season wetted channel extent	Lower with smaller storage capacity	Lower supply of flow from hillslopes to channels
Energy	VII. Stream temperature	Colder in winter and warmer in summer with smaller storage capacity	Small storage capacity promotes shallower hillslope runoff pathways through regions similar to ambient air temperature; big storage capacity promotes deep hillslope runoff pathways through regions with mean annual air temperature
	VIII. Channel shading	Lower with smaller storage capacity in headwaters	Small storage capacity limit growth of plants, decreasing shade adjacent to channel; at large areas, channel is sufficiently wide that riparian vegetation shading becomes less important

directly accelerate egg development in nonperennial streams (Figure 9), so both earlier spawn timing and faster incubation should result in earlier emergence of juveniles. Earlier increases in food availability in sunlit channels support an earlier spring peak in growth potential in intermittent versus perennial streams (Ebersole et al., 2006; Rossi et al., 2022). When the wetted channel dries completely or conditions become lethal, out-migration before the stream dries is the only option for survival. Erman and Leidy (1975) reported that large numbers of *Oncorhynchus mykiss* fry out-migrated from an intermittent stream prior to stream drying, suggesting that these systems contribute to diversity of out-migration timing. In the second year of their study, with more precipitation and perennial summer flows, many juveniles oversummered in the tributary, highlighting the influence of interannual variation in precipitation on life history expression. Oversummering salmonids have also been regularly observed in intermittent streams with remnant pools with adequate water quality that persists through the summer (e.g., Grantham et al., 2012; Hwan

et al., 2018; Obedzinski et al., 2018; Vorste et al., 2020; Woelfle-Eskine et al., 2017). However, wetted habitat area in such channels can be extremely limited, particularly habitats where older (i.e., age 1+ and 2+) fish can rear. In short, these streams can produce large numbers of out-migrating juveniles, but the success of this strategy relies on non-natal growth opportunities elsewhere in the watershed.

In contrast, in perennial streams with year-round flow, more CZ storage of precipitation delays runoff pulses that allow adults to access spawning locations, delaying spawn timing (Figure 3), while cooling groundwater inputs during the spring as eggs incubate (Figure 9) slow development of incubating eggs, delaying emergence relative to the timing of these events in nonperennial streams. However, the slower rate of flow recession in spring and higher mean summer baseflows can support fish that oversummer in the stream and rear for at least one year before out-migration (Kelson & Carlson, 2019). Secondary production increases later than in intermittent streams, which along with sustained recessions and greater channel

shading leads to a later peak in growth potential (Rossi et al., 2022). Perennial flow creates a greater extent of wetted channel and sustained summer rearing environment (both space and water quality) and reduces summer mortality relative to intermittent streams.

Below we delve deeper into these connections and consider how watershed storage capacity influences each of the core events in the life history of Eel River salmonids (e.g., migration and spawn timing, e.g., incubation, growth and foraging, and movement decisions) using Elder Creek and Dry Creek as representative ecological end-members. In particular, we illustrate how CZ conditions lead to flow and temperature regimes that may select for the life history syndromes we describe above. Life history variation among populations in contrasting CZ environments could reflect natural selection (i.e., life history adaptation) or plasticity. Regardless, we posit the habitat conditions in different CZ environments tend to favor the expression of different (and specific) life histories.

## Adult migration and spawning

Migration and spawning require a suitable depth of flow for passage between the ocean and riverine spawning sites as well as suitable hydraulics for spawning once fish arrive at their spawning destination. Subsurface storage deficits at the end of the dry season dictate how much precipitation is needed to elevate winter streamflows in the early wet season (Dralle et al., 2018; Rempe & Dietrich, 2018), which influences the timing of suitable flows for fish migration and spawning. For example, when root-zone storage is fully depleted, flow activation requires twice as much precipitation in Elder Creek as in Dry Creek. Thus, in low-storage capacity watersheds like Dry Creek, we suggest less precipitation is needed to provide suitable flows for migration and spawning, potentially allowing spawning to occur earlier in these systems. In higher storage capacity systems like Elder Creek, a later wet-season flow activation, but more prolonged flow recession, suggests adults may arrive and spawn later—but enjoy a longer duration of suitable spawning conditions. The difference in flow activation between Elder and Dry Creek may vary from hours to weeks depending on their respective storage capacity deficits and initial wet-season rainfall patterns. Variation in subsurface storage capacity, therefore, is likely to generate differences in access and spawn timing during many years, similar to the influence of stream temperature in influencing diversity in this trait among populations (e.g., Lisi et al., 2013).

## Egg incubation

Female salmon build their redds (nests) in the gravel of streambeds. The shape of the redd, the location, and the size of the gravels all differ among species. The developmental rate of eggs also differs among species and is strongly influenced by water temperature (From & Rasmussen, 1991). Temperature variation among streams driven by subsurface properties (see Figure 9) and contributions to discharge from groundwater likely have consequences for egg development rates and fry emergence timing. Riparian vegetation composition and flow volume (thermal mass)—both controlled by features of the CZ—affect the sensitivity of stream water temperature to air temperature and solar radiation (Figure 9). Ephemeral Dry Creek, with its minimal channel shading, warms (and cools) more rapidly than heavily shaded Coastal Belt streams with sustained contributions from groundwater, like Elder Creek. Eggs incubating in redds in the warmer waters of intermittent streams are likely to develop more rapidly, leading to earlier alevin emergence.

In addition to the effect of temperature on egg emergence, salmon redds are at risk of scour and desiccation depending, in part, on the peak discharge of a stream (Holtby & Healey, 1986). Rapid declines in streamflow can potentially cause redds to dry before alevin are able to emerge. Conversely higher peak flows lead to greater risk of redd scour (Holtby & Healey, 1986). In short, in flashy melange streams like Dry Creek, redds are likely also more at risk from scour and desiccation than in more stable streams like Elder Creek (Figure 4).

## Juvenile growth and summer survival

Once salmon fry emerge from the gravels and begin exogenous feeding, differences in CZ structure have implications for the prey production and growth of fish during their early life stages. During the spring months (March–May), streamflow recession coincides with increasing photoperiod and primary and secondary productivity in salmon-bearing food webs of coastal streams like Elder and Dry Creek (Rossi et al., 2022). The timing of streamflow recession relative to ascending food production dictates the seasonality of energetic gains (a function of food concentration and prey capture success) and costs (swimming and basal metabolic costs) for juvenile salmonids, which collectively drive growth potential. However, the relative timing and rate of streamflow recession (Figure 6), water temperature warming (Figure 7), and food web phenology all vary between stream types, driving different seasonal patterns

in growth potential for rearing salmonids (Rossi et al., 2022). All else being equal, streams fed by CZs with low storage capacity will have early, faster recessions and water temperature warming, which will lead to earlier spring increase in juvenile salmonid growth potential, but also an earlier decrease in summer growth potential because very low flows decrease drifting prey and warm water to stressful levels. Whereas in perennial streams fed by CZs with high storage, growth potential for juvenile salmonids will peak later and be sustained longer into the dry season (Rossi et al., 2022).

While growth potential may peak earlier in intermittent streams with low storage potential, these systems also experience an earlier onset of inhospitable conditions for summer rearing salmonids. With warming and hypoxia, and eventual drying and disconnection of the wetted channel network, fish that remain in the stream (as opposed to out-migrating, see next section) can perish (Labbe & Fausch, 2000; Rossi et al., 2022). Importantly, the magnitude of summer mortality varies considerably among years due to interannual variation in rainfall magnitude and the seasonal timing of rainfall delivery (e.g., the date of the last wet-season rainfall Obedzinski et al., 2018). Recent work by Vorste et al. (2020), however, highlights that some intermittent systems provide reliable habitats for juvenile coho rearing. For example, across the geologically complex Russian River watershed in Sonoma County, California, interannual variation in summer survival was high at some sites, but much more stable at other sites, hinting at the importance of CZ properties in influencing the sensitivity of different systems to interannual variation in rainfall and consequences for salmon survival (e.g., Figure 8; see also Moidu et al., 2021).

## DISCUSSION

Our work highlights the explanatory power of broadly applicable, storage-based frameworks across a lithologic gradient in California's Eel River watershed. Building on earlier research, we emphasize that storage capacity controls aspects of flow, temperature, and stream energetics that influence the spatial distribution of stream habitat quantity and quality. We further illustrate how flow and temperature regimes characteristic of our two end-member streams—Elder Creek and Dry Creek—select for different (and specific) salmonid life histories. Below we expand on efforts to measure and model storage capacity, hillslope controls on stream temperature and light environment, and discuss the evolution of salmon and hillslopes over longer timescales.

## Measuring and modeling storage capacity

Storage capacity has predictive potential for ecology, yet it is difficult to measure or estimate; the *in situ* methods deployed at Dry Creek and Elder Creek cannot be realistically deployed at larger scales relevant to managers. Geological maps can be used to extrapolate behaviors over larger scales (under the assumption that rock type is the primary driver of hillslope weathering profiles, e.g., Figure 1), but inferences need to be grounded with data from intensively monitored sites. Alternative approaches to analyzing storage in environments where data are sparse have emerged in recent years. Where discharge data are available, storage–discharge methods and models, or dynamic storage tracking, can provide important insights into subsurface storage processes and their controls on hydrology (Dralle et al., 2018; Kirchner, 2009; Sayama et al., 2011) and flow metrics (Soulsby et al., 2016). Satellite remote sensing methods have emerged as a scalable approach for monitoring plant-driven storage deficits (Wang-Erlandsson et al., 2016), which control flow activation. Maximum observed storage deficits have been correlated with storage capacity as well (McCormick et al., 2021). Geomorphological, ecological, and hydrological model inversion and inferential methods may also provide some insights into the thickness of weathering profiles and water storage capacity (Ichii et al., 2009; Kleidon, 2004; Pelletier et al., 2016; Schenk, 2008). Finally, geophysical methods, such as seismic refraction, have shown promise for understanding ecologically important hillslope-scale storage dynamics with significantly less effort than invasive methods (e.g., Briggs et al., 2018; Holbrook et al., 2014).

## Storage capacity's influence on stream energetics

Although we focus on storage controls on flow regime features that matter for fish, the linkages between storage dynamics and flow behavior have long been studied (e.g., Coutagne, 1948; Hall, 1968; Kirchner, 2009; Sloan, 2000). However, the direct and indirect effects of hillslope storage dynamics on stream energetics are less well understood. We identified three mechanisms by which hillslope storage dynamics could impact stream temperature and light environment. First, storage-controlled plant community composition has consequences for stream shading. Second, flow volumes impact the thermal inertia of water in the channel; all else being equal, lower flows in low-storage Dry Creek result in higher in-channel sensitivity of water temperature to radiation fluxes and air temperature (Webb et al., 2008). Finally, storage dictates flow paths to streams, and because near-surface versus deep flow

paths will have different sensitivities to air temperature, this ultimately will impact the temperature of groundwater and water delivery to channels (Kurylyk et al., 2015). We found water temperature dynamics were consistent with all three of these mechanisms; specifically, the low-storage Dry Creek catchment has flow temperatures that are both hotter and more sensitive to climate than the high storage capacity Elder Creek catchment during the warm summer months. Although we did not determine the relative strengths of these three mechanisms, we did demonstrate potential scale dependence in their impacts. At large scales, channels are wide and therefore hillslope plant communities have less impact on shading. At small scales (headwaters), water has not resided in the channel for long and in-stream temperatures may be more representative of water temperatures being delivered to the channel by the hillslope (Dugdale et al., 2017). Although there have been exciting advances toward incorporating the impacts of flow paths and hillslope processes in stream temperature prediction (Hrachowitz et al., 2010; Leach & Moore, 2015), most efforts focus on climate factors or heat exchange at the stream surface or with channel substrate (Brown, 1969). Increased focus on hillslope processes will be especially important for understanding the fate of headwater refugia during low flow periods (Isaak et al., 2016; Leach & Moore, 2017), where prediction of water temperature sensitivities to climate is highly dependent on hillslope processes (e.g., groundwater flow; Leach & Moore, 2019) and properties (e.g., depth to fresh bedrock; Briggs et al., 2018).

## The evolution of hillslopes and salmon

Geologic history (e.g., Waples et al., 2008), landscape evolution (e.g., Montgomery, 2000) and channel network dynamics (e.g., Stokes & Perron, 2020; Val et al., 2022), and erosional and flood dynamics (Waples et al., 2008), all influence salmon diversity and resilience in the Anthropocene. Here we add another geomorphic component: the CZ. While much practical work has been done in documenting soil thickness and hydrologic properties across landscapes (e.g., the US Natural Resources Conservation Service), little is known about the spatial patterns or controls on the structure, hydrologic properties, and depth of the weathered bedrock zone beneath the soil. Field studies and theoretical analysis have shown that the depth to fresh bedrock (a major control on subsurface water storage capacity) may vary systematically along hillslopes (e.g., Riebe et al., 2016) due to lithologic properties, hydrological processes, weathering, erosion, and tectonics (e.g., Anderson et al., 2013; Brantley & Lebedeva, 2011; Harman & Kim, 2019; Rempe & Dietrich, 2014; Riebe et al., 2016; St. Clair et al., 2015). A common

approach, as illustrated here, has been to study selected hillslopes in a region and then propose models to generalize across watersheds. This is an active research area. Subsurface CZ properties may also be altered over shorter timescales by disturbance events (which may be caused or exacerbated by human activity), such as soil-altering wildfire events (e.g., Moody et al., 2013) or mining (Ross et al., 2021). Watershed hydrologic behavior arises from the collected dynamics of individual hillslopes, whose subsurface capacity to produce recharge and transmit flow downslope dictates the spatial extent of runoff generation and flow recession behavior (Duan & Miller, 1997). Over longer timescales, runoff drives the erosion of channels and the evolution of river networks (e.g., see review and modeling reported in Litwin et al., 2020). Network structure influences the extent of wetted channel (Moidu et al., 2021; Prancevic & Kirchner, 2019) and aquatic habitat (Hwan & Carlson, 2016; Sabo et al., 2010). Additional lithologically influenced hillslope and channel processes that impact habitat include production rate and size of sediment entering channels (Sklar et al., 2017)—including the loading of channels with coarse boulders (Bennett et al., 2016; Roering et al., 2015)—and the upstream migration of steepened reaches (i.e., knickpoints). Propagating knickpoints and boulder-fixed knickpoints occur in the Eel River watershed (e.g., Willenbring et al., 2013) and can lead to barriers to fish passage. Longer term geologic and tectonic processes have been used to explain aspects of salmonid evolution, spatial distribution, and life history strategies (Hassan et al., 2008; Montgomery, 2000; Montgomery et al., 2003; Waples et al., 2008), but the potential indirect effects of these processes on salmonids via the formation of hillslopes, patterns of subsurface storage, and the genesis of river flow–temperature regimes have not been previously identified.

We build on earlier research to emphasize that subsurface CZ diversity likely favors the expression of distinct salmonid life histories and may lead to the emergence of life history syndromes. These include fry dispersing from ephemeral streams early in life and rearing downstream in non-natal habitats prior to ocean entry (Everest, 1973), fish oversummering in intermittent streams with refuge pools and out-migrating the following year (e.g., Hwan et al., 2018), and perennial streams supporting juveniles for one to two years prior to out-migration and, in the case of *O. mykiss*, trout completing the entire life history in the stream (as resident rainbow trout) (e.g., Kelson et al., 2020). Thus, different CZs within a watershed create a mosaic of habitats with different seasonalities and channel characteristics, which likely favor and support distinct life histories.

The success of different life histories will also vary across years due to variation in flow activation and access to tributary breeding habitats, potential for redd scour, spring flow recession and channel warming dynamics, connectivity to downstream non-natal rearing habitat, and disconnectivity of habitats and exposure to lethal temperatures—all of which are consequences of how climate is filtered through the CZ. Across the watershed, maintaining a suite of salmonid populations that differ in their life histories may generate a portfolio effect, wherein the complex of populations is more stable than the individual populations (Schindler et al., 2010). This suggests that the geography of CZ structure may be an important factor contributing to the stability of salmonid population complexes, and that mapping the diversity of CZs across the watershed may be essential to developing successful strategies for sustaining salmon in an era of change.

## CONCLUSION

A lithological gradient across California's Eel River illustrates the power of broadly applicable, storage-based frameworks to explain energetic and flow features of the stream environment that directly affect the behavior and growth of riverine biota, such as salmonids. Different CZs create a mosaic of habitats that likely favor and support different salmonid life histories and may contribute to a stabilizing portfolio effect. Looking beyond the Eel River, our work motivates a deeper study of geological and landscape controls on subsurface water storage capacity. At present, subsurface water supply is poorly mapped beyond shallow soils, despite increasing recognition that storage in deeper layers of weathered bedrock plays an essential role in determining moisture availability and runoff production in water-limited environments. Rapidly advancing methods for estimating and observing subsurface water storage dynamics at large scales present new opportunities for more clearly identifying landscape factors that influence aquatic biota. The linkages between water storage capacity, flow regime, stream energetics, and their consequences for salmonid life history expression highlight the need for a subsurface perspective on how landscapes and their evolution influence salmonid fishes. Better understanding the consequences of different CZs for salmon life history diversity would help managers support resilient salmon populations.

## ACKNOWLEDGMENTS

LiDAR-derived LPI analysis based on services provided by the National Center for Airborne Laser Mapping through the OpenTopography Facility with support from the National Science Foundation under NSF Award

Numbers 1948997, 1948994, and 1948857. We give full credit to Monica Blanchard for the beautiful illustrations in Figures 2 and 4. We acknowledge support from the National Science Foundation CZP EAR-1331940 for the Eel River Critical Zone Observatory. We thank C. Bode for sensor and data assistance. The findings and conclusions in this manuscript are those of the authors and do not necessarily represent the views of the U.S. Fish and Wildlife Service.

## CONFLICT OF INTEREST STATEMENT

The authors declare no conflict of interest.

## DATA AVAILABILITY STATEMENT

Data and code (Dralle, 2023) are available from Zenodo: <https://doi.org/10.5281/zenodo.7562320>.

## ORCID

D. N. Dralle  <https://orcid.org/0000-0002-1944-2103>

W. J. Hahm  <https://orcid.org/0000-0002-9342-8094>

S. M. Carlson  <https://orcid.org/0000-0003-3055-6483>

## REFERENCES

- Anderson, R. S., S. P. Anderson, and G. E. Tucker. 2013. "Rock Damage and Regolith Transport by Frost: An Example of Climate Modulation of the Geomorphology of the Critical Zone." *Earth Surface Processes and Landforms* 38(3): 299–316.
- Anderson, S. P., R. C. Bales, and C. J. Duffy. 2008. "Critical Zone Observatories: Building a Network to Advance Interdisciplinary Study of Earth Surface Processes." *Mineralogical Magazine* 72(1): 7–10.
- Anderson, S. P., F. von Blanckenburg, and A. F. White. 2007. "Physical and Chemical Controls on the Critical Zone." *Elements* 3(5): 315–9.
- Armstrong, J. B., A. H. Fullerton, C. E. Jordan, J. L. Ebersole, J. Ryan Bellmore, I. Arismendi, B. E. Penaluna, and G. H. Reeves. 2021. "The Importance of Warm Habitat to the Growth Regime of Cold-Water Fishes." *Nature Climate Change* 11(4): 354–61.
- Beechie, T., E. Buhle, M. Ruckelshaus, A. Fullerton, and L. Holsinger. 2006. "Hydrologic Regime and the Conservation of Salmon Life History Diversity." *Biological Conservation* 130(4): 560–72. <https://doi.org/10.1016/j.biocon.2006.01.019>.
- Bennett, G. L., S. R. Miller, J. J. Roering, and D. A. Schmidt. 2016. "Landslides, Threshold Slopes, and the Survival of Relict Terrain in the Wake of the Mendocino Triple Junction." *Geology* 44(5): 363–6.
- Berghuijs, W. R., S. J. Gnann, and R. A. Woods. 2020. "Unanswered Questions on the Budyko Framework." *Hydrological Processes* 34(26): 5699–703.
- Bilby, R. E., and P. A. Bisson. 1992. "Allochthonous Versus Autochthonous Organic Matter Contributions to the Trophic Support of Fish Populations in Clear-Cut and Old-Growth Forested Streams." *Canadian Journal of Fisheries and Aquatic Sciences* 49(3): 540–51.

- Bode, C. A., M. P. Limm, M. E. Power, and J. C. Finlay. 2014. "Subcanopy Solar Radiation Model: Predicting Solar Radiation across a Heavily Vegetated Landscape Using Lidar and Gis Solar Radiation Models." *Remote Sensing of Environment* 154: 387–97. <https://doi.org/10.1016/j.rse.2014.01.028>.
- Brantley, S. L., M. B. Goldhaber, and K. V. Ragnarsdottir. 2007. "Crossing Disciplines and Scales to Understand the Critical Zone." *Elements* 3(5): 307–14.
- Brantley, S. L., and M. Lebedeva. 2011. "Learning to Read the Chemistry of Regolith to Understand the Critical Zone." *Annual Review of Earth and Planetary Sciences* 39: 387–416.
- Briggs, M. A., J. W. Lane, C. D. Snyder, E. A. White, Z. C. Johnson, D. L. Nelms, and N. P. Hitt. 2018. "Shallow Bedrock Limits Groundwater Seepage Based Headwater Climate Refugia." *Limnologica* 68: 142–56.
- Brown, G. W. 1969. "Predicting Temperatures of Small Streams." *Water Resources Research* 5(1): 68–75.
- Buoro, M., and S. M. Carlson. 2014. "Life-History Syndromes: Integrating Dispersal through Space and Time." *Ecology Letters* 17(6): 756–67.
- Buttle, J. M. 2016. "Dynamic Storage: A Potential Metric of Inter-Basin Differences in Storage Properties." *Hydrological Processes* 30(24): 4644–53. <https://doi.org/10.1002/hyp.10931>.
- Callahan, R. P., C. S. Riebe, S. Pasquet, K. L. Ferrier, D. Grana, L. S. Sklar, N. J. Taylor, et al. 2020. "Subsurface Weathering Revealed in Hillslope-Integrated Porosity Distributions." *Geophysical Research Letters* 47(15): e2020GL088322. <https://doi.org/10.1029/2020gl088322>.
- Cocking, M. I., J. Morgan Varner, and R. L. Sherriff. 2012. "California Black Oak Responses to Fire Severity and Native Conifer Encroachment in the Klamath Mountains." *Forest Ecology and Management* 270: 25–34.
- Coutagne, A. 1948. "Les variations de débit en période non influencée par les précipitations-le débit d'infiltration (corrélations fluviales internes) 2ème partie." *La Houille Blanche* 5: 416–36.
- Dawson, T. E., W. Jesse Hahm, and K. Crutchfield-Peters. 2020. "Digging Deeper: What the Critical Zone Perspective Adds to the Study of Plant Ecophysiology." *New Phytologist* 226(3): 666–71.
- Dietrich, W. E. 2014. "Eel River Critical Zone Observatory July 2014 Lidar Survey." <https://doi.org/10.5069/G9WH2N2P>.
- Dietrich, W. E. 2015. "Laytonville, CA LiDAR 2015 Airborne LiDAR Survey." <https://doi.org/10.5069/G9WH2N2P>.
- Dott, R. H., and R. H. Shaver, eds. 1974. "Modern and ancient geosynclinal sedimentation." SEPM (Society for Sedimentary Geology). <https://doi.org/10.2110/pec.74.19>.
- Dralle, D. N. 2023. "Salmonid and the subsurface code and data." <https://doi.org/10.5281/zenodo.7562320>.
- Dralle, D. N., W. Jesse Hahm, D. M. Rempe, N. J. Karst, S. E. Thompson, and W. E. Dietrich. 2018. "Quantification of the Seasonal Hillslope Water Storage That Does Not Drive Streamflow." *Hydrological Processes* 32(13): 1978–92. <https://doi.org/10.1002/hyp.11627>.
- Dralle, D. N., N. J. Karst, and S. E. Thompson. 2016. "Dry Season Streamflow Persistence in Seasonal Climates." *Water Resources Research* 52(1): 90–107.
- Duan, J., and N. L. Miller. 1997. "A Generalized Power Function for the Subsurface Transmissivity Profile in Topmodel." *Water Resources Research* 33(11): 2559–62.
- Dugdale, S. J., D. M. Hannah, and I. A. Malcolm. 2017. "River Temperature Modelling: A Review of Process-Based Approaches and Future Directions." *Earth-Science Reviews* 175: 97–113.
- Ebersole, J. L., P. J. Wigington, Jr., J. P. Baker, M. A. Cairns, M. Robbins Church, B. P. Hansen, B. A. Miller, H. R. LaVigne, J. E. Compton, and S. G. Leibowitz. 2006. "Juvenile Coho Salmon Growth and Survival across Stream Network Seasonal Habitats." *Transactions of the American Fisheries Society* 135(6): 1681–97.
- Erman, D. C., and G. R. Leidy. 1975. "Downstream Movement of Rainbow Trout Fry in a Tributary Sagehen Creek, under Permanent and Intermittent Flow." *Transactions of the American Fisheries Society* 104(3): 467–73.
- Everest, F. H. 1973. *Ecology and Management of Summer Steelhead in the Rogue River, Oregon*. Corvallis, OR: State Game Commission.
- Fan, Y. 2019. "Are Catchments Leaky?" *Wiley Interdisciplinary Reviews: Water* 6(6): e1386.
- From, J., and G. Rasmussen. 1991. "Growth of Rainbow Trout, *Oncorhynchus mykiss* (Walbaum, 1792) Related to Egg Size and Temperature." *Dana* 9: 31–8.
- Grant, G. E., and W. E. Dietrich. 2017. "The Frontier beneath Our Feet." *Water Resources Research* 53(4): 2605–9.
- Grantham, T. E., D. A. Newburn, M. A. McCarthy, and A. M. Merenlender. 2012. "The Role of Streamflow and Land Use in Limiting Oversummer Survival of Juvenile Steelhead in California Streams." *Transactions of the American Fisheries Society* 141(3): 585–98.
- Grindley, J. 1968. "The Estimation of Soil Moisture Deficits." *Water for Peace: Water Supply Technology* 3: 241.
- Hahm, W. J., W. E. Dietrich, and T. E. Dawson. 2018. "Controls on the Distribution and Resilience of Quercus Garryana: Ecophysiological Evidence of Oak's Water-Limitation Tolerance." *Ecosphere* 9(5): e02218. <https://doi.org/10.1002/ecs.2.2218>.
- Hahm, W. J., D. N. Dralle, D. M. Rempe, A. B. Bryk, S. E. Thompson, T. E. Dawson, and W. E. Dietrich. 2019. "Low Subsurface Water Storage Capacity Relative to Annual Rainfall Decouples Mediterranean Plant Productivity and Water Use from Rainfall Variability." *Geophysical Research Letters* 46(12): 6544–53. <https://doi.org/10.1029/2019gl083294>.
- Hahm, W. J., D. M. Rempe, D. N. Dralle, T. E. Dawson, and W. E. Dietrich. 2020. "Oak Transpiration Drawn from the Weathered Bedrock Vadose Zone in the Summer Dry Season." *Water Resources Research* 56(11): e2020WR027419.
- Hahm, W. J., D. M. Rempe, D. N. Dralle, T. E. Dawson, S. M. Lovill, A. B. Bryk, D. L. Bish, J. Schieber, and W. E. Dietrich. 2019. "Lithologically Controlled Subsurface Critical Zone Thickness and Water Storage Capacity Determine Regional Plant Community Composition." *Water Resources Research* 55(4): 3028–55.
- Hall, F. R. 1968. "Base-Flow Recessions—A Review." *Water Resources Research* 4(5): 973–83.
- Harman, C. J., M. Sivapalan, and P. Kumar. 2009. "Power Law Catchment-Scale Recessions Arising from Heterogeneous Linear Small-Scale Dynamics." *Water Resources Research* 45(9): W09404. <https://doi.org/10.1029/2008wr007392>.
- Harman, C. J., and M. Kim. 2019. "A Low-Dimensional Model of Bedrock Weathering and Lateral Flow Coevolution in

- Hillslopes: 1. Hydraulic Theory of Reactive Transport." *Hydrological Processes* 33(4): 466–75.
- Hassan, M. A., A. S. Gottesfeld, D. R. Montgomery, J. F. Tunnicliffe, G. K. C. Clarke, G. Wynn, H. Jones-Cox, et al. 2008. "Salmon-Driven Bed Load Transport and Bed Morphology in Mountain Streams." *Geophysical Research Letters* 35(4): W04405.
- Hodge, B. W., M. A. Wilzbach, W. G. Duffy, R. M. Quiñones, and J. A. Hobbs. 2016. "Life History Diversity in Klamath River Steelhead." *Transactions of the American Fisheries Society* 145(2): 227–38.
- Holbrook, W. S., C. S. Riebe, M. Elwaseif, J. L. Hayes, K. B. Reeder, D. L. Harry, A. Malazian, A. Dosseto, P. C. Hartough, and J. W. Hopmans. 2014. "Geophysical Constraints on Deep Weathering and Water Storage Potential in the Southern Sierra Critical Zone Observatory." *Earth Surface Processes and Landforms* 39(3): 366–80. <https://doi.org/10.1002/esp.3502>.
- Holtby, L. B., and M. C. Healey. 1986. "Selection for Adult Size in Female Coho Salmon (*Oncorhynchus kisutch*)."  
*Canadian Journal of Fisheries and Aquatic Sciences* 43(10): 1946–59.
- HRachowitz, M., C. Soulsby, C. Imholt, I. A. Malcolm, and D. Tetzlaff. 2010. "Thermal Regimes in a Large Upland Salmon River: A Simple Model to Identify the Influence of Landscape Controls and Climate Change on Maximum Temperatures." *Hydrological Processes* 24(23): 3374–91.
- Hwan, J. L., and S. M. Carlson. 2016. "Fragmentation of an Intermittent Stream during Seasonal Drought: Intra-Annual and Interannual Patterns and Biological Consequences." *River Research and Applications* 32(5): 856–70.
- Hwan, J. L., A. Fernández-Chacón, M. Buoro, and S. M. Carlson. 2018. "Dry Season Survival of Juvenile Salmonids in an Intermittent Coastal Stream." *Canadian Journal of Fisheries and Aquatic Sciences* 75(5): 746–58.
- Ichii, K., W. Wang, H. Hashimoto, F. Yang, P. Votava, A. R. Michaelis, and R. R. Nemani. 2009. "Refinement of Rooting Depths Using Satellite Based Evapotranspiration Seasonality for Ecosystem Modeling in California." *Agricultural and Forest Meteorology* 149(11): 1907–18.
- Illien, L., C. Andermann, C. Sens-Schönenfelder, K. L. Cook, K. P. Baidya, L. B. Adhikari, and N. Hovius. 2021. "Subsurface Moisture Regulates Himalayan Groundwater Storage and Discharge." *AGU Advances* 2(2). <https://doi.org/10.1029/2021av000398>.
- Isaak, D. J., M. K. Young, C. H. Luce, S. W. Hostetler, S. J. Wenger, E. E. Peterson, J. M. Ver Hoef, M. C. Groce, D. L. Horan, and D. E. Nagel. 2016. "Slow Climate Velocities of Mountain Streams Portend Their Role as Refugia for Cold-Water Biodiversity." *Proceedings of the National Academy of Sciences of the United States of America* 113(16): 4374–9.
- Kelson, S. J., and S. M. Carlson. 2019. "Do Precipitation Extremes Drive Growth and Migration Timing of a Pacific Salmonid Fish in Mediterranean-Climate Streams?" *Ecosphere* 10(3): e02618.
- Kelson, S. J., M. E. Power, J. C. Finlay, and S. M. Carlson. 2020. "Partial Migration Alters Population Ecology and Food Chain Length: Evidence from a Salmonid Fish." *Ecosphere* 11(2): e03044.
- Kirchner, J. W. 2009. "Catchments as Simple Dynamical Systems: Catchment Characterization, Rainfall-Runoff Modeling, and Doing Hydrology Backward." *Water Resources Research* 45(2): W02429.
- Kleidon, A. 2004. "Global Datasets of Rooting Zone Depth Inferred from Inverse Methods." *Journal of Climate* 17(13): 2714–22.
- Klos, P. Z., M. L. Goulden, C. S. Riebe, C. L. Tague, A. Toby O'Geen, B. A. Flinchum, M. Safeeq, et al. 2018. "Subsurface Plant-Accessible Water in Mountain Ecosystems with a Mediterranean Climate." *Wiley Interdisciplinary Reviews: Water* 5(3): e1277.
- Kurylyk, B. L., K. T. B. MacQuarrie, D. Caissie, and J. M. McKenzie. 2015. "Shallow Groundwater Thermal Sensitivity to Climate Change and Land Cover Disturbances: Derivation of Analytical Expressions and Implications for Stream Temperature Modeling." *Hydrology and Earth System Sciences* 19(5): 2469–89.
- Labbe, T. R., and K. D. Fausch. 2000. "Dynamics of Intermittent Stream Habitat Regulate Persistence of a Threatened Fish at Multiple Scales." *Ecological Applications* 10(6): 1774–91.
- Lapides, D. A., W. Jesse Hahm, D. Rempe, W. E. Dietrich, and D. N. Dralle. 2021. "Controls on Streamwater Age in a Saturation Overland Flow-Dominated Catchment." *Water Resources Research* 58: e2021WR031665. <https://doi.org/10.1002/essoar.10508976.1>.
- Leach, J. A., and R. D. Moore. 2015. "Observations and Modeling of Hillslope Throughflow Temperatures in a Coastal Forested Catchment." *Water Resources Research* 51(5): 3770–95.
- Leach, J. A., and D. Moore. 2017. "Insights on Stream Temperature Processes through Development of a Coupled Hydrologic and Stream Temperature Model for Forested Coastal Headwater Catchments." *Hydrological Processes* 31(18): 3160–77.
- Leach, J. A., and R. D. Moore. 2019. "Empirical Stream Thermal Sensitivities May Underestimate Stream Temperature Response to Climate Warming." *Water Resources Research* 55(7): 5453–67.
- Lehner, B., C. R. Liermann, C. Revenga, C. Vörösmarty, B. Fekete, P. Crouzet, P. Döll, et al. 2011. "High-Resolution Mapping of the World's Reservoirs and Dams for Sustainable River-Flow Management." *Frontiers in Ecology and the Environment* 9(9): 494–502. <https://doi.org/10.1890/100125>.
- Lisi, P. J., D. E. Schindler, K. T. Bentley, and G. R. Pess. 2013. "Association between Geomorphic Attributes of Watersheds, Water Temperature, and Salmon Spawn Timing in Alaskan Streams." *Geomorphology* 185: 78–86.
- Litwin, D. G., G. E. Tucker, K. R. Barnhart, and C. J. Harman. 2020. "Groundwater Affects the Geomorphic and Hydrologic Properties of Coevolved Landscapes." *Journal of Geophysical Research: Earth Surface* 127: e2021JF006239.
- Lovill, S. M., W. J. Hahm, and W. E. Dietrich. 2018a. "Drainage from the Critical Zone: Lithologic Controls on the Persistence and Spatial Extent of Wetted Channels during the Summer Dry Season." *Water Resources Research* 54(8): 5702–26. <https://doi.org/10.1029/2017wr021903>.
- Maurer, T., F. Avanzi, S. D. Glaser, and R. C. Bales. 2022. "Drivers of Drought-Induced Shifts in the Water Balance through a Budyko Approach." *Hydrology and Earth System Sciences* 26(3): 589–607.
- McCormick, E. L., D. N. Dralle, W. Jesse Hahm, A. K. Tune, L. M. Schmidt, K. Dana Chadwick, and D. M. Rempe. 2021. "Widespread Woody Plant Use of Water Stored in Bedrock." *Nature* 597(7875): 225–9.

- McCormick, S. D., T. F. Sheehan, B. T. Björnsson, C. Lipsky, J. F. Kocik, A. M. Regish, and M. F. O'Dea. 2013. "Physiological and Endocrine Changes in Atlantic Salmon Smolts during Hatchery Rearing, Downstream Migration, and Ocean Entry." *Canadian Journal of Fisheries and Aquatic Sciences* 70(1): 105–18.
- McDonnell, J. J., J. Evaristo, K. D. Bladon, J. Buttle, I. F. Creed, S. F. Dymond, A. Gordon Grant, et al. 2018. "Water Sustainability and Watershed Storage." *Nature Sustainability* 1(8): 378–9.
- McLaughlin, R. J., W. V. Sliter, N. O. Frederiksen, W. P. Harbert, and D. S. McCulloch. 1994. "Plate Motions Recorded in Tectonostratigraphic Terranes of the Franciscan Complex and Evolution of the Mendocino Triple Junction, Northwestern California." *US Geological Survey Bulletin*, 1997.
- Moidu, H., M. Obedzinski, S. M. Carlson, and T. E. Grantham. 2021. "Spatial Patterns and Sensitivity of Intermittent Stream Drying to Climate Variability." *Water Resources Research* 57(11): e2021WR030314.
- Montgomery, D. R. 2000. "Coevolution of the Pacific Salmon and Pacific Rim Topography." *Geology* 28(12): 1107–10.
- Montgomery, D. R., T. M. Massong, and S. C. S. Hawley. 2003. "Influence of Debris Flows and Log Jams on the Location of Pools and Alluvial Channel Reaches, Oregon Coast Range." *Geological Society of America Bulletin* 115: 78–88.
- Moody, J. A., R. A. Shakesby, P. R. Robichaud, S. H. Cannon, and D. A. Martin. 2013. "Current Research Issues Related to Post-Wildfire Runoff and Erosion Processes." *Earth-Science Reviews* 122: 10–37.
- Müller, M. F., D. N. Dralle, and S. E. Thompson. 2014. "Analytical Model for Flow Duration Curves in Seasonally Dry Climates." *Water Resources Research* 50(7): 5510–31. <https://doi.org/10.1002/2014wr015301>.
- National Marine Fisheries Service. 2014. *Fisheries Economics of the United States, 2012*. Washington, DC: United States Government Printing Office.
- Obedzinski, M., S. N. Pierce, G. E. Horton, and M. J. Deitch. 2018. "Effects of Flow-Related Variables on Oversummer Survival of Juvenile Coho Salmon in Intermittent Streams." *Transactions of the American Fisheries Society* 147(3): 588–605.
- Pedrazas, M. A., W. J. Hahm, M.-H. Huang, D. Dralle, M. D. Nelson, R. E. Breunig, K. E. Fauria, A. B. Bryk, W. E. Dietrich, and D. M. Rempe. 2021. "The Relationship between Topography, Bedrock Weathering, and Water Storage across a Sequence of Ridges and Valleys." *Journal of Geophysical Research: Earth Surface* 126(4). <https://doi.org/10.1029/2020jf005848>.
- Pelletier, J. D., P. D. Broxton, P. Hazenberg, X. Zeng, P. A. Troch, G.-Y. Niu, Z. Williams, M. A. Brunke, and D. Gochis. 2016. "A Gridded Global Data Set of Soil, Intact Regolith, and Sedimentary Deposit Thicknesses for Regional and Global Land Surface Modeling." *Journal of Advances in Modeling Earth Systems* 8(1): 41–65.
- Perkins, J. 2009. "South Fork Eel River, CA: Understanding Terrace Formation and Abandonment." <https://doi.org/10.5069/G93F4MH1>.
- Power, M. E. 2013. "South Fork Eel River, CA: Watershed Morphology." <https://doi.org/10.5069/G9639MPN>.
- Prancevic, J. P., and J. W. Kirchner. 2019. "Topographic Controls on the Extension and Retraction of Flowing Streams." *Geophysical Research Letters* 46(4): 2084–92.
- PRISM Climate Group. 2004. "Prism Rainfall Dataset." <http://prism.oregonstate.edu>.
- Quinn, T. P., S. Hodgson, and C. Peven. 1997. "Temperature, Flow, and the Migration of Adult Sockeye Salmon (*Oncorhynchus nerka*) in the Columbia River." *Canadian Journal of Fisheries and Aquatic Sciences* 54(6): 1349–60. <https://doi.org/10.1139/f97-038>.
- Rempe, D. M., and W. E. Dietrich. 2014. "A Bottom-Up Control on Fresh-Bedrock Topography under Landscapes." *Proceedings of the National Academy of Sciences of the United States of America* 111(18): 6576–81.
- Rempe, D. M., and W. E. Dietrich. 2018. "Direct Observations of Rock Moisture, a Hidden Component of the Hydrologic Cycle." *Proceedings of the National Academy of Sciences of the United States of America* 115(11): 2664–9. <https://doi.org/10.1073/pnas.1800141115>.
- Riebe, C. S., W. Jesse Hahm, and S. L. Brantley. 2016. "Controls on Deep Critical Zone Architecture: A Historical Review and Four Testable Hypotheses." *Earth Surface Processes and Landforms* 42(1): 128–56. <https://doi.org/10.1002/esp.4052>.
- Roering, J. 2006. "Eel River, CA: Landsliding and the Evolution of Mountainous Landscapes." <https://doi.org/10.5069/G9XS5S9P>.
- Roering, J. J., B. H. Mackey, A. L. Handwerger, A. M. Booth, D. A. Schmidt, G. L. Bennett, and C. Cerovski-Darria. 2015. "Beyond the Angle of Repose: A Review and Synthesis of Landslide Processes in Response to Rapid Uplift, Eel River, Northern California." *Geomorphology* 236: 109–31.
- Ross, M. R. V., F. Nippgen, B. L. McGlynn, C. J. Thomas, A. C. Brooks, R. K. Shriner, E. M. Moore, and E. S. Bernhardt. 2021. "Mountaintop Mining Legacies Constrain Ecological, Hydrological and Biogeochemical Recovery Trajectories." *Environmental Research Letters* 16(7): 075004.
- Rossi, G. J., M. E. Power, S. M. Carlson, and T. E. Grantham. 2022. "Seasonal Growth Potential of *Oncorhynchus mykiss* in Streams with Contrasting Prey Phenology and Streamflow." *Ecosphere* 13(9): e4211.
- Sabo, J. L., J. C. Finlay, T. Kennedy, and D. M. Post. 2010. "The Role of Discharge Variation in Scaling of Drainage Area and Food Chain Length in Rivers." *Science* 330(6006): 965–7.
- Salve, R., D. M. Rempe, and W. E. Dietrich. 2012. "Rain, Rock Moisture Dynamics, and the Rapid Response of Perched Groundwater in Weathered, Fractured Argillite Underlying a Steep Hillslope." *Water Resources Research* 48(11): W11528.
- Sayama, T., J. J. McDonnell, A. Dhakal, and K. Sullivan. 2011. "How Much Water Can a Watershed Store?" *Hydrological Processes* 25(25): 3899–908. <https://doi.org/10.1002/hyp.8288>.
- Schenk, H. J. 2008. "The Shallowest Possible Water Extraction Profile: A Null Model for Global Root Distributions." *Vadose Zone Journal* 7(3): 1119–24.
- Schindler, D. E., R. Hilborn, B. Chasco, C. P. Boatright, T. P. Quinn, L. A. Rogers, and M. S. Webster. 2010. "Population Diversity and the Portfolio Effect in an Exploited Species." *Nature* 465(7298): 609–12.
- Schmidt, L., and D. Rempe. 2020. "Quantifying Dynamic Water Storage in Unsaturated Bedrock with Borehole Nuclear Magnetic Resonance." *Geophysical Research Letters* 47(22): e2020GL089600.
- Shapovalov, L., and A. C. Taft. 1954. *The Life Histories of the Steelhead Rainbow Trout (*Salmo gairdneri gairdneri*) and Silver*

- Salmon (*Oncorhynchus kisutch*) with Special Reference to Waddell Creek, California, and Recommendations Regarding Their Management, Vol 98. Sacramento, CA: Department of Fish and Game, State of California.
- Sklar, L. S., C. S. Riebe, J. A. Marshall, J. Genetti, S. Leclere, C. L. Lukens, and V. Merces. 2017. "The Problem of Predicting the Size Distribution of Sediment Supplied by Hillslopes to Rivers." *Geomorphology* 277: 31–49.
- Sloan, W. T. 2000. "A Physics-Based Function for Modeling Transient Groundwater Discharge at the Watershed Scale." *Water Resources Research* 36(1): 225–41.
- Soulsby, C., C. Birkel, and D. Tetzlaff. 2016. "Modelling Storage-Driven Connectivity between Landscapes and Riverscapes: Towards a Simple Framework for Long-Term Ecohydrological Assessment." *Hydrological Processes* 30(14): 2482–97.
- St. Clair, J., S. Moon, W. S. Holbrook, J. T. Perron, C. S. Riebe, S. J. Martel, B. Carr, C. Harman, K. Singha, and D. deB Richter. 2015. "Geophysical Imaging Reveals Topographic Stress Control of Bedrock Weathering." *Science* 350(6260): 534–8.
- Staudinger, M., M. Stoelzle, S. Seeger, J. Seibert, M. Weiler, and K. Stahl. 2017. "Catchment Water Storage Variation with Elevation." *Hydrological Processes* 31(11): 2000–15. <https://doi.org/10.1002/hyp.11158>.
- Stokes, M. F., and J. T. Perron. 2020. "Modeling the Evolution of Aquatic Organisms in Dynamic River Basins." *Journal of Geophysical Research: Earth Surface* 125(9): e2020JF005652.
- Sturrock, A. M., S. M. Carlson, J. D. Wikert, T. Heyne, S. Nusslé, J. E. Merz, H. J. W. Sturrock, and R. C. Johnson. 2019. "Unnatural Selection of Salmon Life Histories in a Modified Riverscape." *Global Change Biology* 26(3): 1235–47. <https://doi.org/10.1111/gcb.14896>.
- Sykes, G. E., C. J. Johnson, and J. Mark Shrimpton. 2009. "Temperature and Flow Effects on Migration Timing of Chinook Salmon Smolts." *Transactions of the American Fisheries Society* 138(6): 1252–65. <https://doi.org/10.1577/t08-180.1>.
- Thornton, M. M., R. Shrestha, Y. Wei, P. E. Thornton, S. Kao, and B. E. Wilson. 2020. "Daymet: Daily Surface Weather Data on a 1-km Grid for North America, Version 4." <https://doi.org/10.3334/ORNLDaac/2129>.
- Tune, A. K., J. L. Druhan, J. Wang, P. C. Bennett, and D. M. Rempe. 2020. "Carbon Dioxide Production in Bedrock beneath Soils Substantially Contributes to Forest Carbon Cycling." *Journal of Geophysical Research: Biogeosciences* 125(12): e2020JG005795.
- Val, P., N. J. Lyons, N. Gasparini, J. K. Willenbring, and J. S. Albert. 2022. "Landscape Evolution as a Diversification Driver in Freshwater Fishes." *Frontiers in Ecology and Evolution* 9: 975.
- Vorste, R. V., M. Obedzinski, S. N. Pierce, S. M. Carlson, and T. E. Grantham. 2020. "Refuges and Ecological Traps: Extreme Drought Threatens Persistence of an Endangered Fish in Intermittent Streams." *Global Change Biology* 26(7): 3834–45.
- Wald, J. A., R. C. Graham, and P. J. Schoeneberger. 2013. "Distribution and Properties of Soft Weathered Bedrock at Less Than 1 m Depth in the Contiguous United States." *Earth Surface Processes and Landforms* 38(6): 614–26.
- Wang-Erlandsson, L., W. G. M. Bastiaanssen, H. Gao, J. Jägermeyr, G. B. Senay, A. I. J. M. Van Dijk, J. P. Guerschman, P. W. Keys, L. J. Gordon, and H. H. G. Savenije. 2016. "Global Root Zone Storage Capacity from Satellite Based Evaporation." *Hydrology and Earth System Sciences* 20(4): 1459–81.
- Waples, R. S., G. R. Pess, and T. Beechie. 2008. "Evolutionary History of Pacific Salmon in Dynamic Environments." *Evolutionary Applications* 1(2): 189–206.
- Webb, B. W., D. M. Hannah, R. Dan Moore, L. E. Brown, and F. Nobilis. 2008. "Recent Advances in Stream and River Temperature Research." *Hydrological Processes: An International Journal* 22(7): 902–18.
- Westhoff, M. C., H. H. G. Savenije, W. M. Luxemburg, G. S. Stelling, N. C. Van de Giesen, J. S. Selker, L. Pfister, and S. Uhlenbrook. 2007. "A Distributed Stream Temperature Model Using High Resolution Temperature Observations." *Hydrology and Earth System Sciences* 11(4): 1469–80.
- Willenbring, J. K., N. M. Gasparini, B. T. Crosby, and G. Brocard. 2013. "What Does a Mean Mean? The Temporal Evolution of Detrital Cosmogenic Denudation Rates in a Transient Landscape." *Geology* 41(12): 1215–8.
- Woelfle-Erskine, C., L. G. Larsen, and S. M. Carlson. 2017. "Abiotic Habitat Thresholds for Salmonid over-Summer Survival in Intermittent Streams." *Ecosphere* 8(2): e01645.
- Yarnell, S. M., E. D. Stein, J. Angus Webb, T. Grantham, R. A. Lusardi, J. Zimmerman, R. A. Peek, B. A. Lane, J. Howard, and S. Sandoval-Solis. 2020. "A Functional Flows Approach to Selecting Ecologically Relevant Flow Metrics for Environmental Flow Applications." *River Research and Applications* 36(2): 318–24.
- Yoshiyama, R. M., and P. B. Moyle. 2010. *Historical Review of Eel River Anadromous Salmonids, with Emphasis on Chinook Salmon, Coho Salmon and Steelhead*. Davis, CA: University of California, Center for Watershed Sciences.

**How to cite this article:** Dralle, D. N., G. Rossi, P. Georgakakos, W. J. Hahm, D. M. Rempe, M. Blanchard, M. E. Power, W. E. Dietrich, and S. M. Carlson. 2023. "The Salmonid and the Subsurface: Hillslope Storage Capacity Determines the Quality and Distribution of Fish Habitat." *Ecosphere* 14(2): e4436. <https://doi.org/10.1002/ecs2.4436>